OPTICALLY STIMULATED LUMINESCENCE DOSIMETRY USING AL_2O_3:C MICRO CRYSTALS

Clarita Saldarriaga Vargas

Work placement report

External supervisors:
Luana de Freitas Nascimento, M.Sc.
Emiliano D'Agostino, Ph.D.

Academic supervisor:
Alexandre Maître, Ph.D.

University of Limoges
Faculty of Sciences and Technology
Master in Advance Ceramic Materials
Limoges, France
September 2011

Université de Limoges | FACULTÉ DES SCIENCES ET TECHNIQUES

Abstract

The present report resulted from a masters student internship developed in the Belgian Nuclear Research Centre SCK•CEN with facilities in Mol, Belgium.

This work studied the Optically Stimulated Luminescence (OSL) response of carbon-doped aluminium oxide (Al_2O_3:C) powder dosimetric detectors to beta and gamma radiation. The OSL detectors were prepared in the form of flattened drops of about 2-3 mm in diameter by mixing the Al_2O_3:C powder with a photo-curable polymer that hardens when illuminated with strong UV light. The powder consists on Al_2O_3:C micro crystals with a maximum grain size of 38 μm with high OSL sensitivity to ionizing radiation like beta particles, gamma rays and X-rays. The samples were prepared in small sizes in order to increase the spatial resolution of the detectors.

OSL measurements were performed using the automated Risø TL/OSL reader system model TL/OSL-DA-20 produced by Risø National Laboratory, Denmark. This system is equipped with blue LEDs emitting at 470 nm to stimulate the samples and a bi-alkali EMI 9235QA photomultiplier tube with Hoya U-340 filters to detect the emitted luminescence of the samples. Irradiations of the detectors were performed using beta and gamma rays from a $^{90}Sr/^{90}Y$ and a ^{60}Co source respectively.

Different measurements were carried out to characterize the OSL response of the Al_2O_3:C powder detectors. Firstly, the variation of the OSL response with the amount of powder used per detector was measured. From this test, the minimum amount of powder necessary to perform a dosimetric measurement with the Risø reader was estimated. Then, several dosimetric properties of powder samples were assessed and were compared with those obtained for two other available forms of Al_2O_3:C detectors: a single macro crystal and Luxel™ detectors. In this sense, some tests of the linearity of the OSL response versus dose curve were done using beta doses from 126 mGy to 20 Gy and gamma doses from 100 mGy to 10 Gy. This range of doses was used to account for the doses commonly measured in medical dosimetry. From these tests, differences in the OSL response of powder samples for beta and gamma irradiations were analysed. Also, changes in the OSL sensitivity of powder and Luxel detectors with the accumulated dose were followed for accumulated doses below 28 Gy of beta. Furthermore, fading effects of powder and Luxel detectors were examined for periods of time of up to 3 days between irradiation and readout. The reproducibility of the OSL measurements using the Risø reader and Luxel detectors was also checked.

The results obtained from these measurements corroborated the valuable high OSL sensitivity of the Al_2O_3:C powder to ionizing radiation. A small amount of just 10 μg of powder per detector showed to be enough to perform a dosimetric measurement of a beta dose of 126 mGy using the Risø reader. Respect to their dosimetric properties, powder detectors presented an OSL response for $^{90}Sr/^{90}Y$ beta radiation comparable to that one of Luxel detectors, showing a linear behaviour from 126 mGy until about 10 Gy. Respect to the OSL response to other radiation qualities, when irradiating with ^{60}Co gamma rays, the dose range with linear behaviour of the OSL response was larger for powder samples (~ 0,1 - 10 Gy) than for Luxel detectors (~ 0,1 - 7,5 Gy). Besides this, the OSL response of powder samples irradiated with ^{60}Co gamma rays was higher than that one of samples irradiated with $^{90}Sr/^{90}Y$ beta rays, which may be partly due to the charged nature of beta radiation. Additionally, regarding changes in the OSL sensitivity with the accumulated dose, powder and Luxel detectors showed opposite effects for accumulated doses below 30 Gy of beta. More results and important observations about these measurements are mentioned in this text. At the end, several tests to perform in the future are proposed in order to refine the obtained results and go farther in the study of the dosimetric properties of the Al_2O_3:C powder detectors.

About SCK•CEN

SCK•CEN is one of the largest research centers in Belgium. Throughout its more than 50 years of experience, SCK•CEN has earned a reputation as a center of excellence for research in the field of peaceful applications of nuclear science and technology and ionizing radiation. Its research activities are concentrated in six main research domains: advanced nuclear systems, nuclear materials, fusion technology, radiation protection, disposal of radioactive waste and societal aspects of nuclear research. All research activities are concentrated into three scientific institutes, which are further organized into expert groups devoted to specific research topics and projects.

The present work was framed in the project of Optically Stimulated Luminescence (OSL) Dosimetry of the Radiation Protection, Dosimetry and Calibration (RDC) expert group at the institute for Environment, Health and Safety (EHS).

The RDC expert group conducts research and offers services related to the measurement and characterization of ionizing radiation doses in different environments. The main research lines are situated in the fields of personal dosimetry and dosimetric techniques, medical dosimetry applications and neutron, space, retrospective and internal dosimetry. The group has a solid expertise in thermoluminescence (TL) and optically stimulated luminescence (OSL) dosimetry techniques and Monte Carlo simulations and it provides services for other SCK•CEN groups and for external customers.

SCK•CEN
Environment, Health and Safety
Radiation protection, Dosimetry and Calibration
Boeretang, 200
2400, Mol
Belgium

Luana de Freitas Nascimento, M.Sc.
Tel.: +32 (0)14 33 27 19
ldfnasci@sckcen.be

Emiliano D'Agostino, Ph.D.
Tel.: +32 (0)14 33 21 39
edagosti@sckcen.be

CONTENTS

List of Figures

1 INTRODUCTION

The exposure to ionizing radiation of human beings could be potentially harmful if no adequate control is implemented. When radiation interacts with matter, it transfers part or total of its energy to the atoms of the medium. This energy, related to the radiological quantity of absorbed dose, could be high enough to detach electrons from its atoms, breaking chemical bonds important for the continuity of cells life.

The field of physics who deals with the measurement and calculation of the absorbed dose and its related radiological quantities is the *radiation dosimetry.* More specifically, personal dosimetry is the subspecialty of radiation dosimetry in charge of the monitoring of workers that are exposed to ionizing radiation, both in industrial and clinical environments. Similarly, medical dosimetry focuses on the measurement, estimation and delivery optimization of patients dose levels associated with medical procedures, typically in diagnostic radiology and cancer treatment with radiation therapy, using ionizing radiation.

The devices used to measure and monitor the radiation absorbed dose are called *dosemeters.* In radiation medicine, accurate and high spatial resolution are some of the required characteristics for a dosimetric system in order to ensure that the patient is not overexposed and that the exposure occurs in the desired region, so that the probability of developing secondary malignancies and other damaging effects related to the undesired irradiation of healthy tissues can be reduced. Similarly, in personal dosimetry, high performance and cost-effective personal dosimetric systems are desired in order to monitor occupational radiation doses and provide information for health surveillance and treatment in case of accidental exposures.

In the 1990s, carbon-doped aluminium oxide (Al_2O_3:C) was introduced as an ionizing radiation sensitive material with potential dosimetric properties to fulfil the necessities in these fields. Due to its Thermo-Luminescence (TL) and Optically Stimulated Luminescence (OSL) properties, Al_2O_3:C has been widely used in personal dosimetry (McKeever, 2001) and is now expanding its potentialities into the fields of medical (Akselrod, et al., 2007) (Yukihara, et al., 2010) (Pradhan, et al., 2008) (Cygler, et al., 2009) and space dosimetry (Yukihara, et al., 2006a). Al_2O_3:C currently dominates the commercial OSL-based personal dosimetry market, but it has also been used for in vivo real-time radiotherapy dosimetry (Aznar, et al., 2004) (Polf, et al., 2004) (Huston, et al., 2001) and passive space dosimetry of heavy-charged particles (Yukihara, et al., 2006b).

The Al_2O_3:C currently used in dosimetry is produced in the form of single crystals. Single crystal detectors are usually cut into square or round shapes of few millimetres of dimensions. In order to solve problems of different sensitivities to ionizing radiation between similar single crystal detectors, Al_2O_3:C single crystals may be crushed to produce Al_2O_3:C powder (micro crystals) with homogeneous sensitivity that can be later used to prepare other forms of OSL Al_2O_3:C detectors. A commercial dosimetric tape using Al_2O_3:C powder has been produced by Landauer Inc. and is used in several dosimetric systems like Luxel™, InLight™ and nanoDot™ from the same company.

The present work, issued from a masters student internship in the Radiation, Dosimetry and Calibration expert group at SCK•CEN, has focused on the study of dosimetric properties of the Al_2O_3:C powder form. A protocol to prepare OSL detectors using Al_2O_3:C micro crystals at different concentrations has been implemented taking into account the relevant needs for a dosimetric detector in the fields of medical and personal dosimetry. Some dosimetric properties of the prepared powder

detectors like linearity of the OSL response versus dose curve, stability of the OSL signal after irradiation, accumulated dose effects, dependence of the OSL response on radiation quality and accuracy of the measurements, were compared with those obtained from detectors cut from the commercial Al_2O_3:C dosimetric tape from Landauer Inc. (Luxel™ detectors) and from an Al_2O_3:C single crystal. Also, the minimal amount of Al_2O_3:C powder necessary to perform a dosimetric measurement using powder detectors was investigated.

First, this work mentions some basic aspects of radiation dosimetry, optically stimulated luminescence dosimetry and characteristics of the Al_2O_3:C in order to have an overview of the topic. Then, it describes the experimental details and method employed during measurements and presents the results obtained for each type of detector. The analysis and discussion of results are shown at the same time that these ones are presented. Finally, a general conclusion of the work and its perspectives are exposed.

2 OBJECTIVES OF THE PROJECT

The development of this project seeks to achieve the following objectives:

- Develop a protocol to prepare optically stimulated luminescence detectors (OSLDs) using Al_2O_3:C micro crystals (Al_2O_3:C powder) at different concentrations, taking into account the relevant needs for a dosimetric detector in the fields of medical and personal dosimetry;
- Determine the minimal amount of Al_2O_3:C powder necessary to perform a dosimetric measurement with the available equipment at SCK•CEN;
- Compare the optically stimulated luminescence (OSL) response of prepared powder detectors with the response of other available forms of Al_2O_3:C detectors: a single macro crystal and Luxel™ detectors. This implies characterizing dosimetric properties like linearity of the OSL response versus dose curve, accumulated dose effects, fading of the OSL signal, dependence of the OSL response on radiation quality, accuracy of the measurements, etc.

The fulfil of these objectives will not only increase the experience and knowledge of the RDC group in OSL dosimetry, but it will also bring up new ideas for a current PhD project within the RDC group related to real time in-vivo dosimetry and for future projects.

3 BASIC CONCEPTS

3.1 Radiation dosimetry

When radiation interacts with matter, it transfers part or total of its energy to the atoms of the medium. The way in which this process occurs depends on the medium, the type of incident radiation and its energy. When the energy of the incident radiation is too high, the transferred energy may be enough to detach electrons from atoms causing their ionization. In these cases we are talking about ionizing radiation. It includes, among others, gamma rays, X-rays, alpha and beta particles, neutrons, protons and heavy ions.

As mentioned before, a primary radiological quantity related to the transferred energy by the radiation is the *absorbed dose (D)*. It is equal to the energy imparted *E* in a medium per unit of mass *m* by ionizing radiation (see Equation (1)) and it is measured in joules per kilogram, represented by the equivalent SI unit *gray* (Gy).

$$D = \frac{dE}{dm} \qquad (1)$$

The field of physics who deals with the measurement and calculation of the absorbed dose and its related radiological quantities is the *radiation dosimetry*.

The use of ionizing radiation has allowed great progress in many areas of medicine. In radiotherapy, ionizing radiation is used as part of cancer treatment to damage malignant cells. In radiology, medical experts use this radiation in some medical imaging and diagnosis techniques such as in x-ray radiographies and CT scans (computed tomography scans). The doses delivered to patients (which may include a tissue, an organ, a tumour or the whole body) depend, among other factors, on the medical procedure. In radiological procedures doses may go from fractions of milligray (mGy) as for a chest radiograph (~ 0.14 mGy), passing through several tens milligray as for X-ray CT scans (multiple scan average dose ~ 20-100 mGy), to up to several hundred milligray as for a complete fluoroscopy procedure (real-time moving imaging technique using x-rays). However, much higher dose levels are required to treat malignant diseases during radiation therapy. In some type of cancers, total preventive doses using photon beams are typically around 60 Gy and they are delivered in fractions of 1.8-2 Gy per day (Yukihara, et al., 2011 p. 224) (Jursinic, 2007). In total body irradiation (TBI), a radiation therapy procedure used primarily as part of the preparative regimen for bone marrow transplantation, total x-ray doses go from 2 Gy to up to 14 Gy (Gore, et al., 1996) (Mangili, et al., 1999). For reference, a whole body dose of 4.5 Gy of an acute exposure (a radiation exposure occurring in a short period of time) is fatal in 50% of the exposed individuals (assuming no medical care). Also, it is known from a number of epidemiological studies that secondary malignancies and other damaging effects such as cataract formation, skin erythema and infertility can occur due to the doses inevitably received by healthy tissues during the treatment.

Now well, it is not surprising that a subspecialty of dosimetry has focused on the measurement, estimation and delivery optimization of patients dose levels associated with medical procedures using ionizing radiation. This subspecialty is called *medical dosimetry*. Also, an analogous subspecialty responsible for the monitoring of the dose received from people when they are occupationally exposed to ionizing radiation (as *e. g.* medical staff, workers in nuclear facilities) is introduced and it is called *personal dosimetry*. With the same purpose, some dose limits for workers, students and members of the

public are recommended by international organizations like IAEA (*International Atomic Energy Agency*), ICRP (*International Commission on Radiological Protection*) and Euratom.

Along with this, the development and improvement of techniques for an effective dose assessment is also an important activity. For the measurement and monitoring of radiation dose some devices known as *dosemeters* are used. A dosimeter is capable of providing a reading that is related to the absorbed dose deposited in its sensitive volume (sensitive material) by the ionizing radiation. These devices may be in the form of passive dosimeters (record of the exposure for a determined period of time) or of active dosimeters (real-time reading of dose and dose rate). Passive dosimeters may include film badges, TLDs (Thermo-Luminescent Dosimeters) and OSLDs (Optically Stimulated Luminescent Dosimeters) (see Figure 3.1).

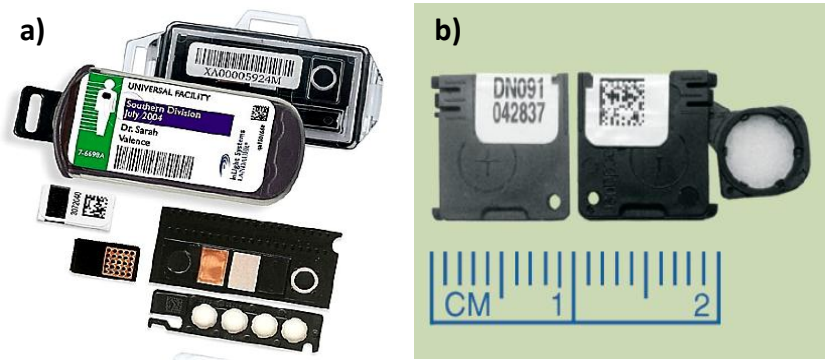

Figure 3.1. Two passive Al_2O_3:C OSL dosimeters from Landauer Inc: a): the InLight ™ system with four Al_2O_3:C detectors used in personal dosimetry and b): the nanoDot™ used in medical dosimetry.

3.1.1 General characteristics of dosimeters

Some characteristics of dosimeters relevant in personal and medical dosimetry are described below.

- Precision: it specifies the reproducibility of the measurements under similar conditions and can be estimated from the data obtained in repeated measurements. It is related to random errors due to fluctuations in instrumental characteristics, ambient conditions and the stochastic nature of radiation. High precision is associated with small standard deviations.
- Dose sensitivity: is associated to the readout signal intensity per unit of radiation dose.
- Linearity: constant dose sensitivity throughout the dose range provides a linear response. This is desirable to facilitate the calibration and interpretation of the reading.
- Background: or *zero-dose reading* is the value of the readout signal when there is no delivered dose (zero-dose). This signal is not caused by the irradiation of the dosimeter and depends on each detector; therefore it should be subtracted from any dosimeter reading.
- Dose range: it is determined by the lower and upper dose limits. The lower dose limit is usually estimated to be the dose necessary to double the instrumental background reading (Attix, 1986 p. 279). The upper limit is manifested by a decrease in the dose sensitivity to an unacceptable value.
- Size: the spatial resolution of a detector is determined by its physical size. A dosimeter with good spatial resolution (small size) allows the accurate determination of dose distributions in small regions characterized by large dose heterogeneities and/or significant dose gradients. Small sized dosimeters are possible due to materials with high dose sensitivities.

- Stability before irradiation: the properties of a dosimeter should remain stable with time until it is used. Effects of temperature, atmospheric oxygen or humidity and light can cause a gradual change in the dose sensitivity or background of the dosimeter.
- Stability after irradiation: the latent reading of the dosimeter may be unstable, suffering *fading* losses during the time interval between irradiation and readout. Harsh ambient conditions of elevated temperature or humidity or direct sunlight may intensify this effect.
- Energy dependence: it is related to the dependence of the response of the dosimeter upon the quality of the incident radiation (type and energy). An important requirement for the use of a material as a dosimetric detector in medical and personal dosimetry is to be approximately tissue equivalent. As the energy deposited in a material by radiation depends on its mass energy absorption coefficient and this one also depends on the effective atomic number of the material (Z_{eff}), materials with Z_{eff} near that of human tissue (Z_{eff} = 7.6) are desired. A detector with Z_{eff} near 7.6 will behave similarly as tissue when interacting with ionizing radiation, which means that it will absorb the same dose as tissue (where a measurement may take place) when exposed to the same radiation field. However, no material such as those used in OSLD or TLDs is tissue equivalent and, as a consequence, energy dependence is an important characteristic of these systems that requires correction.
- Directional dependence: is the variation of the readout response with the angle of incidence of radiation. Dosimeters usually exhibit directional dependence due to their constructional design, physical size and the energy of the incident radiation.
- Reusability: it depends on how easy it is to restore a dosimeter to its original condition. Some dosimeters show a shift in their sensitivity depending on the irradiation/dose-readout history. They are said to present *memory effects*.

An ideal dosimetric system would present, among other characteristics, high precision and sensitivity, linear response for a wide range of doses, small size, low background, no significant fading and flat energy dependence. It should be possible to be reused without memory effects and its readout procedure should be fast and simple. Carbon-doped aluminium oxide (Al_2O_3:C) is almost an exceptional material meeting several of these specifications. As mentioned before, due to its TL (Thermoluminescence) and OSL (Optically Stimulated Luminescence) properties it is widely used in personal dosimetry and is now expanding its potentialities into the fields of medical and space dosimetry.

3.2 Optically Stimulated Luminescence

Optically stimulated luminescence (OSL) is the luminescence emitted from an irradiated insulator or semiconductor when it is exposed to light. Even if the OSL phenomenon can be observed in materials like glasses, plastics and biological materials, in practice, most used OSL materials are crystals with lattice defects. As we will see, these defects are the key factor of the OSL properties from such materials.

The stimulated luminescence process can be explained in terms of the available energy levels structure of some insulators and semiconductors (see Figure 3.2). There are three possible bands where charge carriers involved in the OSL process can be found:

- The *conduction band*, where electrons have enough energy to move freely within the atomic lattice of the material. It may be empty in the case of an insulator or partially filled in conductors and semiconductors.
- The *valence band*, with lower energies than the conduction band. It may be filled in insulators and conductors or partially filled in a semiconductor, being the electrons bounded to individual atoms.
- The *forbidden band*, with some intermediate energy levels between the conduction band and the valence band called *trap centers* (T) and *recombination centers* (R), which are available due to the presence of defects such as vacancies or impurities within the material.

A crystal defect is classified as a trap center if the defect is able to capture a charge carrier and reemit it back to the band it came from. A trap center can capture and hold charge carriers in an electrical potential for usefully long periods of time.

A crystal defect where carriers of opposite sing can be captured resulting in an electron/hole recombination is classified as a recombination center. A recombination center can be located at either electron traps or hole traps and they can be luminescent (with emission of light when electrons and holes recombine) or not.

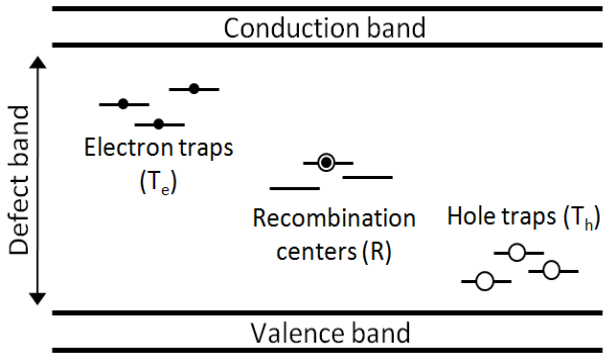

Figure 3.2. Representation of energy bands in an insulating crystal and localized energy levels introduced by defects.

When ionizing radiation interacts with an insulating crystal a redistribution of charge within the crystal takes place. The absorption of energy in the material causes the ionization of valence electrons creating electron/hole pairs. The excited electrons are freely moving in the crystal until they are captured by an electron trap center T_e (see Figure 3.3) or by a recombination center R. A hole generated in the valence band is captured by either a hole trap center T_h or by a recombination center R. This redistribution of charge continues during the exposure to ionizing radiation and the amount of trapped charge is proportional to the total radiation exposure.

When irradiation is over, the trapped charge can be released by exposing the crystal to either heat (thermal stimulation) or light (optical stimulation). In the second case, light is used to cause the relaxation of the system back to its equilibrium condition. During this process, electrons and holes are freed into the conduction and valence band respectively, then a subsequent transition to a radiative recombination center occurs and finally a flux of light is emitted (luminescence). The intensity of the emitted luminescence is proportional to the amount of trapped charge and hence to the absorbed dose. If heating is applied to release the trapped charges, the luminescence is called thermo luminescence (TL). If light exposure is the releasing agent, the light emission is called optically stimulated luminescence (OSL).

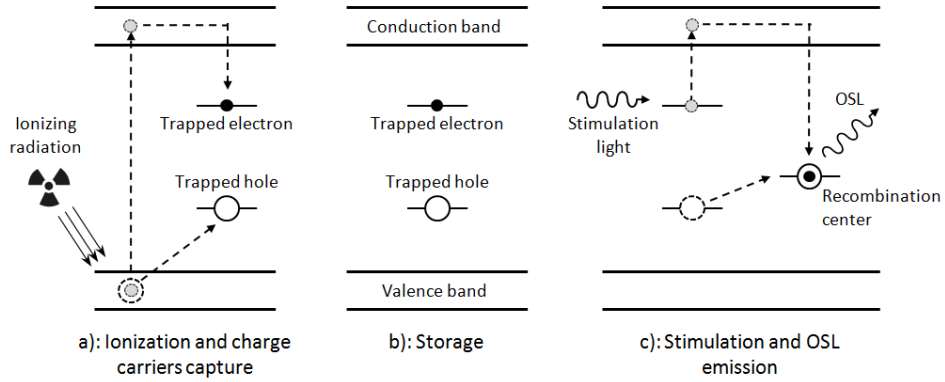

Figure 3.3. Simplified illustration of different stages involved in the OSL process: (a) electron/hole pair production due to the exposure to ionizing radiation and trapping of charge carriers; (b) latency period characterized by a metastable concentration of charge carriers captured at defects in the crystal and (c) stimulation of the crystal with light, leading to recombination of electron-hole pairs and emission of light (OSL).

The luminescence lifetime depends on the type of traps and recombination pathways. Once an electron or a hole is trapped, it can spontaneously recombine without being released by any light/heat stimulation. The deeper the trap, the more energy is needed to reach it and stimulate the charge carrier. Shallow trapped charges, due to their proximity to the conducting band, can recombine under ambient temperatures. Dosimetric traps are energetically deep enough to hold charge at room temperature for long periods of time, but are not so deep that the charge cannot be released by illumination with visible light (Markey, et al., 1996).

It is important not to confuse the OSL with the related phenomenon of photoluminescence (PL) that can be stimulated from similar materials, but which is generally not dependent on a previous irradiation of the sample. PL is the excitation, via the absorption of light, of an electron in a crystal defect within the material, resulting in excitation of the electron from the ground state of the defect to an excited state. Relaxation back to the ground state results in the emission of luminescence and the intensity of this one is proportional to the concentration of excited defects.

In OSL, the intensity of the stimulated luminescence is associated to the rate at which the crystal returns to the equilibrium. The rate at which the equilibrium is re-established is a function of the concentration of trapped charge and, in the simplest case, the rate is linearly proportional to the trapped charge concentration. Normally, the intensity of the luminescence is monitored as a function of time, resulting in a characteristic luminescence-versus-time curve. The integral of this curve is thus related to the trapped charge concentration, and this, in turn, is related to the absorbed dose. This is the basis for the use of OSL in radiation dosimetry.

3.2.1 Main modes of stimulation

The luminescence signal decay and the algorithm to calculate the absorbed dose depend on the method used for optical stimulation. The stimulating light source can be visible, ultra-violet or infra-red. Most popular stimulation schemes are illustrated in Figure 3.4.

Figure 3.4 (a) shows the *continuous wave OSL* (CW-OSL) stimulation mode. In this mode the power of the stimulating light is kept constant and the OSL signal is monitored continuously during the stimulation period. Figure 3.4 (b) shows the *linearly modulated OSL* (LM-OSL) stimulation mode. This method uses linearly ramped stimulation intensity while the OSL is measured. Figure 3.4 (c) presents the third mode or *pulsed OSL* (POSL) stimulation, in which the stimulation light is pulsed and the OSL is measured only between pulses.

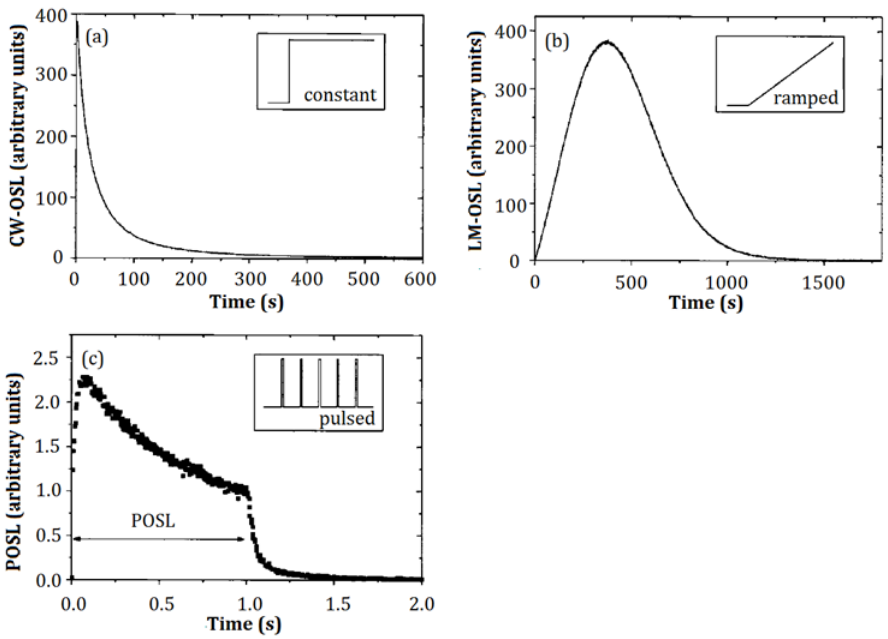

Figure 3.4. Experimental data illustrating three main OSL readout modes: (a) CW-OSL, (b) LM-OSL, and (c) POSL (from (Bøtter-Jensen, et al., 2003 p. 6)).

To calculate the absorbed dose using the OSL decay curve it is necessary to develop an algorithm. This algorithm takes into consideration the quality of the ionizing radiation, the mode of stimulation, the dosimetric material and the type of defect/impurity where the electron/hole was trapped. The material used in this work is the Al_2O_3:C and it will be better explained in the following sections.

3.3 α-Al_2O_3

Corundum or α-aluminium oxide (α-Al_2O_3) is the most common form of crystalline alumina. It is well known for its abrasive and refractory properties due to its high hardness (8-9 in Mohs scale) and melting point (~ 2044 °C), but it is also an important material for many optical and electronic applications. It is used as gain medium in solid-state lasers, in optical windows, as substrate for epitaxial growth in semiconductor industry and even more recently as a radiation detector (Akselrod, et al., 1990).

In α-Al_2O_3, oxygen ions nearly form a hexagonal close-packed structure with aluminium ions filling two-thirds of the octahedral interstices. Each Al^{3+} center is octahedral and is surrounded by six O^{2-} ions (Figure 3.5). In terms of crystallography, corundum adopts a trigonal Bravais lattice with a space group of R-3c (No. 167 in the International Tables).

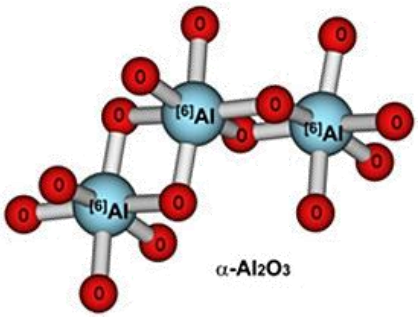

Figure 3.5. Crystalline structure of α-Al_2O_3.

3.4 Al_2O_3:C

The introduction of carbon doped Al_2O_3:C as a material for TL dosimetry (Akselrod, et al., 1990) and OSL dosimetry (Akselrod, et al., 1999) opened the possibilities for high sensitivity dosimetry. In 1995 McKeever *et al.* showed that Al_2O_3:C possesses a TL sensitivity 40-60 times greater than other common used dosimetric materials like LiF:Mg,Ti (McKeever, et al., 1995). Few years later Bøtter-Jensen *et al.* demonstrated that Al_2O_3:C presents even a higher radiation sensitivity when using OSL techniques (Bøtter-Jensen, et al., 1997). Today, Al_2O_3:C OSLD applications are rapidly expanding into the fields of personal (McKeever, 2001) and space dosimetry (Yukihara, et al., 2006a) and more recently into the field of medical dosimetry (Akselrod, et al., 2007) (Yukihara, et al., 2010) (Pradhan, et al., 2008) (Cygler, et al., 2009). Some of the dosimetric characteristics of Al_2O_3:C exploited in these fields are its high sensitivity to several types of ionizing radiation, its capacity of storage of dose information for long periods of time after irradiation and its fairly easy readout technique.

As the OSL intensity depends on the trap concentration of the dosimetric material, growing aluminium oxide crystals with high concentration of lattice defects is of special interest for dosimetry. For Al_2O_3 crystals, carbon impurities have shown to be excellent promoters of the formation of oxygen vacancies (Akselrod, et al., 1993).

Al_2O_3 is usually produced using Czochralksi, Verneuil or Stepanov techniques at temperatures higher than 2050 °C. Its carbon-doped form is grown in a strong reducing atmosphere in the presence of graphite to favour the formation of oxygen ion vacancies while substitutions of Al^{3+} anions by carbon C^{2+} anions occurs in the crystal lattice (Figure 3.6) (Agersnap-Larsen, 1997). This vacancies, associated to F and F^+ centers (neutral and charged oxygen vacancies) (Evans, 1995), play the important role in the OSL sensitivity of alumina since they act as trapping and luminescent recombination centers for both holes and electrons.

The existence of F^+ centres, in particular, is essential for an efficient OSL emission. F^+ centres work as luminescent recombination centres for electrons, resulting in excited F-centres (F*) and a subsequent luminescence due to its relaxation into F-centers (see Equation (2)) (Summers, 1984). The relaxation of the F* center is the responsible of the 410–420 nm (blue) peak centred band emission of Al_2O_3:C stimulated luminescence (see Figure 3.7a) (Akselrod, et al., 1990) and it possesses a lifetime of 35 ms at room temperature (Summers, 1984).

However, although to a lesser extent, excited F^+ centers are also involved in the OSL emission. These centers, probably formed from recombination of holes (h^+) into F centers, emit at 325 nm (UV) during their relaxation into ground state F^+ centers, but with a lifetime shorter than 7 ns (see Equation (3)) (Evans, 1995) (Yukihara, et al., 2011 p. 85).

$$F^+ + e^- \rightarrow F^* \xrightarrow{\tau=35ms} F + \hbar\omega_{420\ \mathrm{nm}} \qquad (2)$$

$$F + h^+ \rightarrow F^{+*} \xrightarrow{\tau<7ns} F^+ + \hbar\omega_{325\ \mathrm{nm}} \qquad (3)$$

A more detailed description of the absorption and emission processes associated with F and F^+ centers can be read in (Evans, 1995), (Bøtter-Jensen, et al., 2003) and (Yukihara, et al., 2011 p. 85).

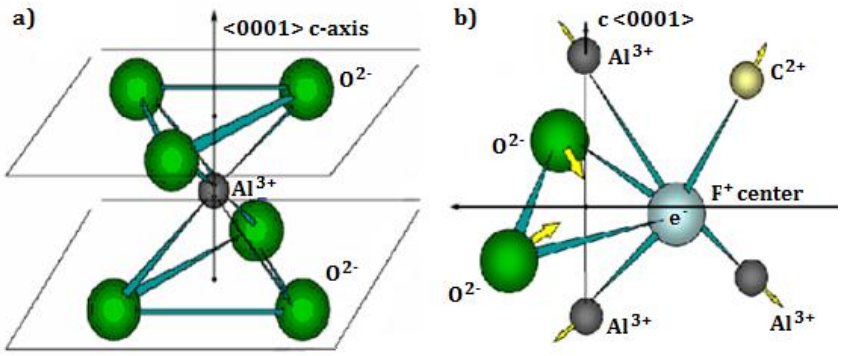

Figure 3.6. a) Crystalline structure of Al_2O_3; b) Oxygen vacancy in Al_2O_3:C (from (de Freitas Nascimento, 2007 p. 21)).

Stimulation of the luminescence of Al_2O_3:C can be done using a broad spectrum of light from 400 to 700 nm with a peak of stimulation at 475 nm (Bøtter-Jensen, et al., 1996) (Markey, et al., 1995). From Figure 3.7 (b) one can see that the OSL intensity from Al_2O_3:C increases when decreasing the stimulation wavelengths.

Usually green stimulation is used for OSL measurements of Al_2O_3:C because it efficiently stimulates the OSL signal while facilitating discrimination of stimulation and detection light bands. The use of blue stimulation is also possible and it offers advantages such as faster readout times (i.e. OSL curves with faster decay) and higher initial OSL intensity. However, in spite of these advantages there is experimental evidence that blue stimulation introduces some problems not usually observed with green stimulation, including higher residual OSL intensities (or background signal) due to stimulation of charge carriers from deeper traps, residual OSL intensities depending on the previous absorbed dose history of detectors and incomplete bleaching when detectors are bleached with yellow or green light (Umisedo, et al., 2010).

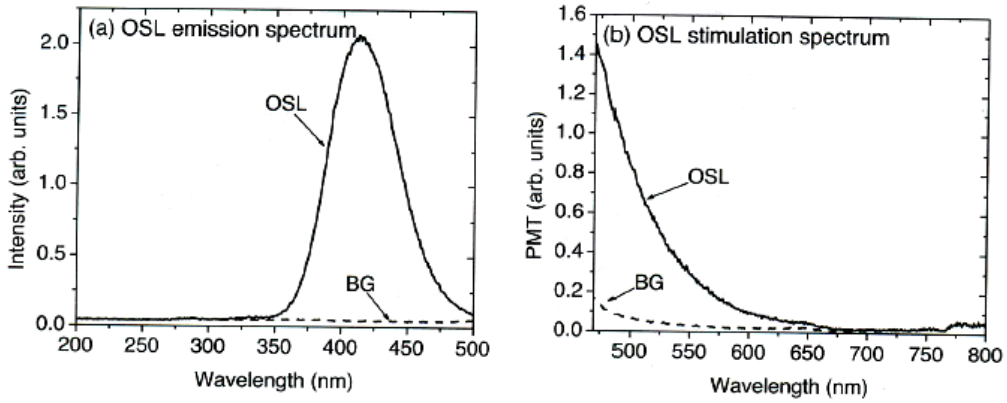

Figure 3.7. (a) Emission and (b) excitation spectrum of the OSL of Al_2O_3:C (from (Yukihara, et al., 2011 p. 78)). BG indicates the background signal obtained after the OSL signal was erased by optical stimulation (zero-dose signal).

4 EXPERIMENTAL DETAILS AND METHODS

4.1 Materials

4.1.1 Al_2O_3:C OSL detectors

The Al_2O_3:C currently used in dosimetry is produced in the form of single crystals. Single crystal detectors are usually cut into square or round shapes of few millimetres of dimensions. As they can be annealed to reset their sensitivity (clean-up of full traps), Al_2O_3:C single crystals present the advantage of being useful for almost indefinitely periods of time. However, single crystal detectors have shown to possess different sensitivities to ionizing radiation even when they come from the same batch due to a non-uniform distribution of defects within the stem crystal. To address this problem, Al_2O_3:C crystals may be crushed, mixed and sieved into the desired particle size range to produce Al_2O_3:C powder with homogeneous sensitivity, which can later be used to prepare other forms of OSL detectors.

In this work three different forms of Al_2O_3:C detectors were used: a single crystal, Luxel™ detectors and prepared powder detectors.

4.1.1.1 Single crystal detector

The single crystal detector was produced by the Crystal Growth Division of Landauer Inc. in Stillwater, USA. It has a square prism shape of 1 millimetre wide and 2 millimetres long (Figure 4.1 and Figure 4.2a). Its small size allows it to be attached to the optical fibers used in real time radiotherapy dosimetry probes (Gaza, et al., 2004) (Marckmann, et al., 2006) (Andersen, et al., 2008).

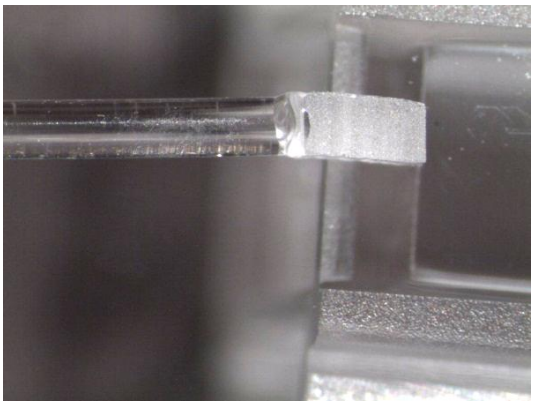

Figure 4.1. Al_2O_3:C single crystal coupled to a PMMA optical fiber for radiotherapy online dosimetry.

4.1.1.2 Luxel™ detectors

Our Luxel™ detectors (OSL detectors as those used in the Luxel™, InLight™ and nanoDot™ dosimetric systems from Landauer Inc.) are round and thin detectors of 4.5 millimetres diameter obtained from a commercial Al_2O_3:C dosimetric tape from Landauer Inc. (Figure 4.2a). Currently Luxel^{TM} systems are used as personal dosimeters in several countries. To produce the tape from which they are made, the Al_2O_3:C powder is mixed with a polymeric binder and coated onto a roll of polyester film. The aluminium oxide layer is about 0.13 mm thick and is packed between polyester foils 0.05 mm thick (top) and 0.08 mm thick (bottom).

4.1.1.3 Powder detectors

Powder detectors were prepared using an Al_2O_3:C powder also provided by Landauer Inc. The powder has a grain size below 38 micrometres, which means that grains of smaller sizes are also encountered into it.

For an easy manipulation of the powder during measurements and trying to avoid the contamination of the Risø reader with it, a method to hold the powder was implemented. First, solutions of powder and water were prepared and small drops of the solutions were put between small and thin glass discs. This method did not seem to be appropriate since glass discs tended to disperse the OSL signal from the powder grains avoiding the correct and reproducible detection of the signal. After this, some viscous substances like agarose gel and lubricant oil over metallic sample holders were tested to avoid the use of glass discs for carrying the powder but, in this case, they showed to be sensitive to ionizing radiation and presented their own OSL response. Finally a transparent photo-curable polymer was tested and none of the mentioned drawbacks appeared.

Preparation:

Powder detectors were prepared mixing Al_2O_3:C powder with a photo-curable polymer. This polymer hardens only after being illuminated with a strong UV light source (AKTIPRINT T UT51002, from TECHNIGRAF GmbH). It is not sensitive to ionizing radiation, it does not show any OSL response and it does not absorb light in the luminescence wavelength of Al_2O_3:C.

The polymer consists of the following components:

1. 2 ml of Tetrahydrofurfuryl acrylate from Sigma Aldrich (408271).
2. 3 ml of Di(trimethylolpropane) tetraacrylate from Sigma Aldrich (408360).
3. 25 mg of 2-Hydroxy-2-methylpropiophenone 97% pure from Sigma Aldrich (40565-5), which is the UV photo-initiator.

Samples of different powder concentrations and volumes were prepared using the following protocol:

1. Weighing of the powder using a high precision balance (standard deviation of 0,02 mg) and an Eppendorf tube as container.
2. Pipetting of the polymer inside the Eppendorf tube using a micro-pipette.
3. Shaking of the Eppendorf tube for ~ 2 minutes in the vortex to homogenise the solution.
4. Measurement of small volumes of solution using a micro-pipette of 1 - 10 µl.
5. Exposure of the little drops of solution to UV light to harden the polymer.

Each small drop is an Al_2O_3:C powder OSL detector (Figure 4.2b) and its size depends on the volume of solution used. Drops of 1 µl present a diameter of about 2 to 3 millimetres.

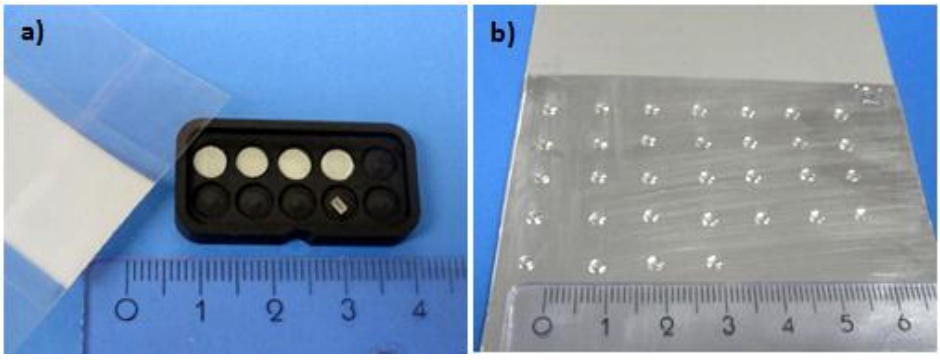

Figure 4.2. Al_2O_3:C detectors: (a) the single crystal with four Luxel™ detectors and the Luxel™ tape and (b) 32 powder detectors of 1 µl.

4.1.2 Risø OSL reader

Most of OSL measurements during this project where done using the automated Risø TL/OSL reader system model TL/OSL-DA-20 produced by Risø National Laboratory in Denmark. This system is capable of carrying out sequences of OSL measurements and irradiations, as well as TL measurements and heating procedures of multiple samples. As the reader was used only for OSL measurements, only the components involved in our OSL procedures are mentioned.

The Risø reader includes three basic systems: (i) an optical stimulation system, (ii) a photon detector unit and (iii) a beta irradiator facility (Figure 4.3). These systems are mounted over a dark chamber, where samples are positioned in a turntable (the carrousel) with capacity for up to 48 samples.

The optical stimulation unit consists of an array of blue light emitting diodes (LEDs) arranged in 4 clusters each one of 7 LEDs. The clusters are placed in a ring between the turntable and the detection system, just above one sample position in order to illuminate the sample/detector and stimulate its luminescence. The LEDs emit at 470 nm (FWHM = 20 nm) and the whole set give a total light power density of approximately 50 $mW.cm^{-2}$ at sample position (about 20 mm below the LEDs).

For the detection of the stimulated luminescence a photomultiplier tube (PMT) is positioned over the stimulation unit. A PMT is a high sensitive light transducer capable of converting an electromagnetic signal (photons) into an amplified and low noise electric signal (electrons). The PMT of the Risø reader is a bi-alkali EMI 9235QA PMT, with an extended UV response with maximum detection efficiency between 300 and 400 nm.

In order to be able to measure the emitted luminescence which is about 10^{18} orders of magnitude lower than the intensity of the stimulation light, detection filters must be used to prevent scattered stimulation light from reaching the PMT and the spectral stimulation and detection windows must be well separated. For this, a detection filter (Hoya U-340) is placed between the PMT and the stimulated sample, blocking the scattered stimulation light and isolating specific OSL emission bands characteristics of the OSL material (see Figure 3.7). This filter transmits both the emission from the F-center (420 nm) and the F^{+}-center (UV). Also, a stimulation filter (GG-420 green long pass filter) is incorporated in front of each blue LED cluster. This filter also reduces the amount of directly scattered blue light from reaching the PMT and allows selecting the stimulation wavelength or band that is optimum for a specific OSL material (see Figure 3.7).

Irradiations with beta particles are also possible by means of a $^{90}Sr/^{90}Y$ ceramic source (particles with a maximum energy of 2.27 MeV) placed above the carrousel. The exposure of a sample to beta radiation is controlled by a pneumatic system that turns up or down the source. The delivered dose is determined by the amount of time of exposure, being 1 second the minimum exposure time. The distance between the source and the sample is 5 mm and a 0.125 mm beryllium window acting as vacuum interface is located between the irradiator and the measurement chamber. At the moment of irradiations the dose rate at sample position was of 126 ± 8 $mGy.s^{-1}$.

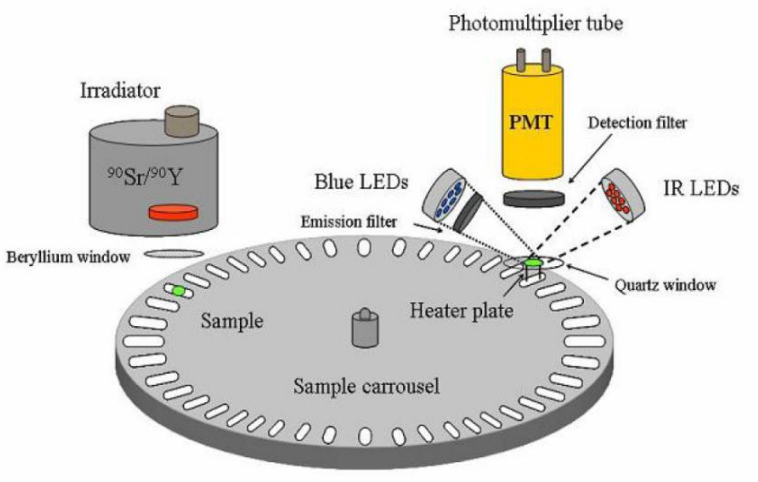

Figure 4.3. Schematic of the automated Risø TL/OSL reader system (from user manual). Other components that were not used during our experiments are also included in this illustration.

4.1.3 Apollo OSL reader

Another OSL reader developed by the Radiation Dosimetry and Calibration (RDC) expert group at SCK•CEN was used. The main reason of using another OSL reader system is related to the possibility of using other stimulation light band for comparison of results with blue stimulation.

The Apollo reader uses a green LED with main peak at 505 nm (B3b-443-B505 from Daina Electronics Co., Ltd) as stimulating light source. Unlike the Risø system, the Apollo works in a transmission mode, which means that the detector is illuminated by one side and by the other side the stimulated luminescence is detected. The detection of the OSL is done using a bi-alkali photomultiplier tube from Electron Tubes Inc. The light emitted by the LED is cleaned up with a long-pass filter (GG-420) and the PMT is protected by two U-340 band-pass filters to measure only a part of the ultraviolet spectrum emitted by the detectors. As the Apollo does not allow changing the power of the stimulation light and after some technical problems with it, OSL measurements with this device were limited to just few tests at the beginning of this work.

4.2 OSL protocol

All OSL measurements followed a basic protocol:

- Bleaching of detectors to remove any residual signal;
- Irradiation of detectors with a radioactive source for a specific time to deliver the desired dose;
- Readout of the OSL signal with a specific stimulation light band and intensity and detection system.

4.2.1 Bleaching

Bleaching of all detectors was done using the blue light of the Risø reader at 100% of the maximal power (~ 50 $mW.cm^{-2}$). Luxel™ detectors and single crystal were bleached during at least 15 minutes, but longer bleaching times were used depending on the previous received dose of the detectors. For powder detectors, only 90 seconds of exposure to blue light were enough to bleach them completely. When a different bleaching protocol is used, it will be specified in the results section of the test.

4.2.2 Irradiation

The $^{90}Sr/^{90}Y$ source of the Risø system was used for all irradiations with beta particles. Electrons emitted from this source have a maximum energy of 2.27 MeV. The dose rate in air at samples position at the moment of irradiations was of 126 $mGy.s^{-1}$.

For gamma irradiations, a ^{60}Co source of the Calibration Laboratory of SCK•CEN (KAL) was used. This source emits gamma photons in the 1.17 and 1.33 MeV emission lines and its dose rate was of 1548 $mGy.h^{-1}$ (±10 $mGy.h^{-1}$ depending on the date of irradiation). Gamma irradiations were performed at 21 °C in air, with a distance between source and samples of 75 cm.

Doses from about 100 mGy to 60 Gy were tested with both sources. However, in most of the cases the range of interest was between 100-126 mGy and 10-20 Gy because it is a wide range of doses involved in radiation therapy. Before and after irradiation of detectors, handling of samples was carried out inside of a dark room to avoid the release of the OSL signal due to stimulation with an external source of light.

4.2.3 Readout

Regarding reading instrumentation, almost all measurements were done using the Risø reader (blue stimulation light) in continuous wave mode. At the beginning the Apollo reader (green stimulation light) was also used for the linearity test of Luxel™ detectors. However, as it did not offer the possibility of changing the power of the stimulation light and after having some technical problems with the power supply and the detection system, it was not possible to keep using this reader and therefore only blue stimulation (Risø reader) was used for the subsequent measurements.

The power of the stimulation light as well as the stimulation times used in measurements depend on each test, so they will be specified later when presenting the results.

4.3 Analysis

After reading the OSL signal, the collected data was used to calculate the total integrated OSL intensity (I_T) and the initial integrated OSL intensity (I_P) of the signal. These are commonly used quantities to account for the measured luminescence.

To estimate the total intensity I_T, all the counts (C) obtained from the PMT during the measurement should be integrated (total counts), then normalized by the total reading time (t_f) and then the background of the signal (B) should be subtracted from this result (see Equation (4),Equation (5) and Figure 4.4). Usually, measurements using the CW mode are done until achieving the background level of the OSL signal (i.e. until the dosimetric traps are empty). In accordance with this, total OSL intensity refers to the integrated OSL intensity estimated using the stimulation time t_f needed to drop the signal until background levels. As mentioned before, background signal do not provide any information of the absorbed dose and depends on each detector. In order to have comparable results by referencing the integrated OSL signals to the same zero-dose base, the background of each detector (usually the signal during the last seconds of stimulation) should be removed from the dosimetric calculations.

To estimate the initial or peak OSL intensity a similar calculation is performed, but in this case only the first seconds of the stimulation time (from t=0 until $t=t_P$) are taken into account for the sum (see Equation (6)). Different behaviours of the dose response may be found when using the initial OSL intensity instead of the total OSL intensity. Thus, both quantities are usually estimated and compared in OSL dosimetric measurements.

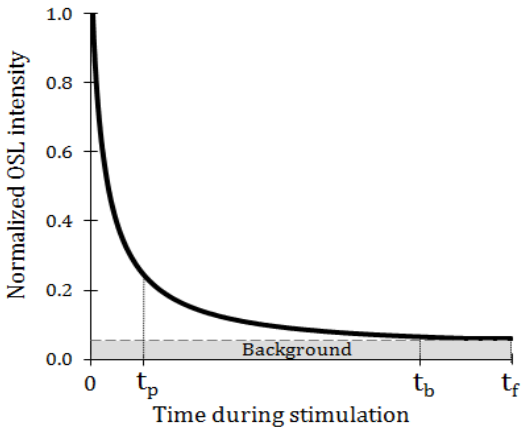

Figure 4.4. Typical OSL curve when using the continuous wave stimulation mode (CW-OSL).

The formulas used to calculate the mentioned OSL intensities and background quantities are shown below.

$$B = \frac{1}{t_f - t_b} \sum_{i=t_b}^{t_f} C_i \tag{4}$$

$$I_T = \frac{1}{t_f} \sum_{i=0}^{t_f} C_i - B \tag{5}$$

$$I_P = \frac{1}{t_p} \sum_{i=0}^{t_p} C_i - B \tag{6}$$

Besides luminescent intensities, other two quantities were used in the analysis of results. The linearity factor *f(D)* (Equation (7)) in function of the absorbed dose *D*, which allows assessing the degree of linearity of the dose response curve; and the relative sensitivity $S(D_a)$ (Equation (8)) in function of the accumulated dose D_a, which will be helpful to identify changes in sensitivity within the accumulated dose of the detectors. These quantities are defined as follows:

$$f(D) = \frac{I(D)/D}{I_0/D_0} \tag{7}$$

$$S(D_a) = \frac{I(D_a)}{I_{ref}} \tag{8}$$

Where I_0 is the integrated OSL intensity obtained for an absorbed dose D_0 in the linear range of the dose response and I_{ref} is the integrated OSL intensity measured for the minimum accumulated dose tested in the experiment.

4.4 Tests

Different measurements were carried out for the study of the OSL response of the mentioned types of Al_2O_3:C detectors.

First measurements include some preliminary linearity tests using Luxel™ detectors done mainly to get familiarized with the OSL protocol and the equipment (both the Apollo and the Risø). As the tests were repeated later, they will not be described.

After this, linearity tests using beta and gamma irradiated Luxel™ detectors were performed. Linearity tests were done using both beta particles and gamma rays in order to compare the response of the detectors to ionizing radiation of different quality. Both green and blue stimulation were used and different stimulation light powers were tested when measuring with the Risø reader (blue light). Doses from 100 mGy to up to 60 Gy were delivered to the detectors.

In the sequence, powder detectors of different concentrations were prepared according to the protocol mentioned in section 4.1.1.3. Hereafter only the Risø reader was used for measuring the OSL. Some tests to estimate the minimum amount of powder necessary to perform a dosimetric measurement and tests of the variation of the OSL response within powder concentration of equally sized samples (drops of same volume) were performed. Trying to prepare equal powder detectors, the reproducibility of samples preparation was assessed. In addition, linearity tests were carried out using beta doses from 126 mGy to 15 Gy and gamma doses from 100 mGy to 10 Gy.

Afterwards, Luxel detectors and powder samples underwent similar experiments. These include reproducibility tests to estimate the precision of the samples at different experimental conditions (e.g. stimulation light power, delivered dose, type of detector, etc.), sensitivity tests to check if there were changes in the OSL response of the detectors depending on their dose history, linearity tests using new and used (i.e. pre-irradiated) detectors irradiated with beta to see if the OSL versus dose curve presents a new shape due to variations in the OSL response of detectors and finally, fading tests to appraise the stability of the OSL signal over time after delivery of dose.

Regarding the single crystal, measurements using this detector were more limited once only one unity was available for measurements. The single crystal underwent a reproducibility test in the Risø and linearity tests using both beta and gamma irradiations, for doses from 100 mGy to up to about 13 Gy.

4.5 Time planning

This project was developed according to the following time planning of activities. Details about each stage are mentioned all over this work.

Table 1. Time planning of the general stages accomplished during this work.

Stage	March	April	May	June	July	August
Literature study						
Recognition tests using Luxel detectors						
Preparation of powder samples						
OSL measurements with all detectors						
Analysis of the data						
Preparation of the report						

5 RESULTS AND DISCUSSION

5.1 Measurements using Luxel™ detectors

5.1.1 Linearity test using $^{90}Sr/^{90}Y$-beta particles

The decay of the luminescence of a Luxel™ detector irradiated with 1,26 Gy of beta using continuous wave green stimulation (Apollo reader) is shown in Figure 5.1. The ordinate axis represents the photons counted every second (counts per second or cps) by the PMT and the abscissa is the time during stimulation with light.

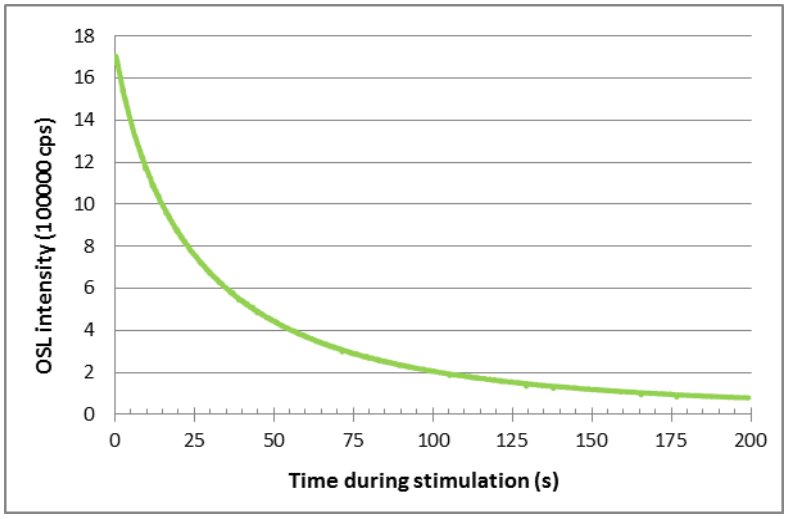

Figure 5.1. OSL decay curve of a Luxel detector irradiated with 1.26 Gy of beta using the Apollo reader.

Figure 5.2 shows the linearity test of Luxel detectors using the Apollo reader. Each point represents the average of the integrated initial OSL intensity of different sets of two detectors. Only the first ten seconds of the peak curve of each detector were taken into account for calculation of the initial OSL intensity (see Equation (6)). Luxels were bleached during one day using day light with a UV filter and then they were irradiated with beta particles using the $^{90}Sr/^{90}Y$ source of the Risø reader.

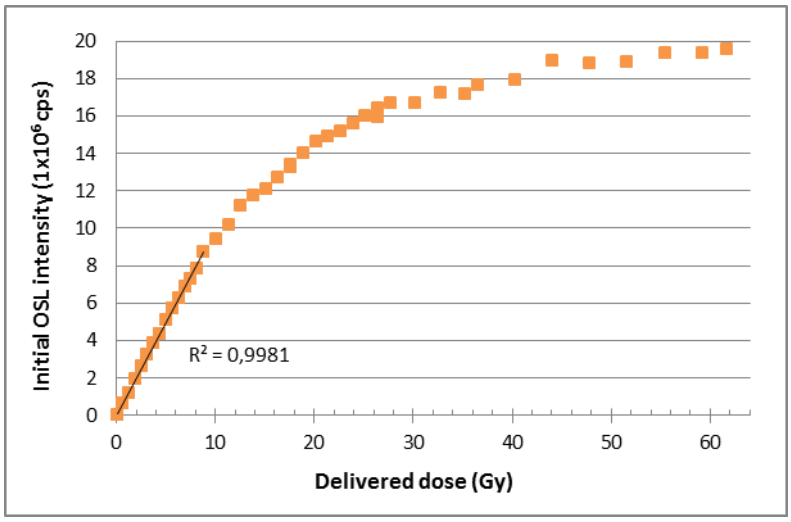

Figure 5.2. Linearity test of Luxel™ detectors irradiated with beta, using the Apollo reader.

Having linear readout signals for the interested range of doses is desired in dosimetry applications since linear OSL responses allow performing fast calibrations of dosimeters and easy estimations of doses from the calibration curve. The test of Figure 5.2 shows that a linear behaviour goes from the minimum delivered dose (126 mGy) to up to about 9 Gy and then it starts a strong decaying of the OSL response of the detectors. This is not the expected behaviour since it is known that Luxel™ detectors start exhibiting saturation effects above 50 Gy (Bøtter-Jensen, et al., 2003 p. 75) (Yukihara, et al., 2004) (Yukihara, et al., 2011 pp. 132-136), which means that something else is precipitating the loss of response at higher doses. Causes of saturation of the OSL signal imposed by the dosimetric material itself are related to an exhaustion of available dosimetric trapping centers to harbour charge carriers responsible of the OSL generation. At high doses dosimetric traps are filled rapidly and electrons freed in the conduction band by a subsequent irradiation (i. g. higher doses) are not able to get trapped in any dosimetric center. As a consequence, different higher doses show similar OSL intensities and a plateau appears in the dose response curve of the dosimetric material, making impracticable the determination of a delivered dose from such a calibration curve and limiting thus the dose range.

However, the upper limit of the useful dose range of a dosimeter may also be imposed by external instrumental limitations. This is the case in this linearity test in which the saturation of the OSL signal of the dosimetric system (detector + OSL reader) was not related with the detector itself but with the OSL detection system. In fact, the Apollo reader only offers one stimulation light power to illuminate the detector. The stimulation light intensity seemed to be too high, causing a faster depletion of the dosimetric traps and thus a higher initial OSL intensity. The PMT was not able to measure such as strong intensity and therefore saturation in the readout signal appeared.

Then, taking advantage of the possibility of the Risø reader of varying the stimulation light power, appropriate stimulation intensities (using blue light instead of green light) to read our Luxel detectors were investigated for doses from 126 mGy to up to 20 Gy. Three linearity tests from 126 mGy to 10 Gy with beta particles using different stimulation intensities of blue light (different percentages of the maximum light power of the set of blue LEDs) are exposed in Figure 5.3. These tests were done using the same detector, applying several sequences of blue bleaching, beta irradiation and OSL readout. The total stimulation time of each test was different as the decaying rate of the OSL curve depends on the stimulation light intensity. The chart shows that at 90% of the maximum power (~ 45 $mW.cm^{-2}$) an early nonlinear behaviour of the dose response due to saturation of the detection system (the PMT) appears above 2 Gy. At 50% (~ 25 $mW.cm^{-2}$) the curve is linear until about 5 Gy and then it starts showing a slight negative curvature (sublinearity). Then 10% was tested but the OSL response was very similar to that one at 50%, which means that there are no observable effects of saturation of the PMT below 50% of the maximum power for the evaluated dose range.

A remark from these tests is that the slight negative curvature above 5 Gy only appears in the dose response curves at 50% and 10% if the data points are estimated using the total integrated OSL intensity (as in Figure 5.3). When using the initial integrated OSL intensity with an integration time of few seconds, the dose response exhibits a different behaviour above 5 Gy where it becomes supralinear. Thus, it brings up that the shape of the OSL response versus dose curve may depend to some extent on the integration time taken into account to calculate the points of the curve. This can be better observed in Figure 5.4, where different dose response curves estimated from different integration times are illustrated. In this case the linearity test was done until 20 Gy of beta dose, the stimulation light was used at 10% of the maximum LEDs intensity and the total stimulation time was of 1800s.

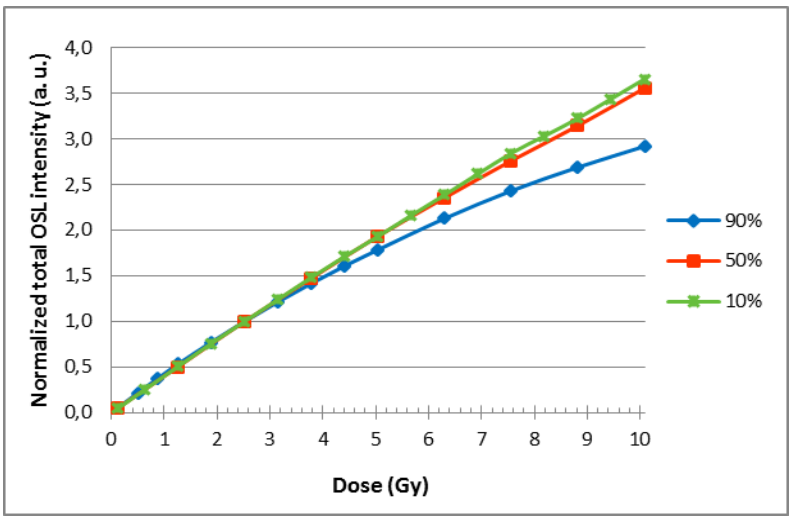

Figure 5.3 Linearity tests of Luxel detectors up to 10 Gy with beta using three different intensities of blue stimulation light. Values of each test are normalized to the total integrated OSL intensity at 2,52 Gy.

The OSL response versus dose curve using the total OSL intensity (Figure 5.4b) exhibits a linear-sublinear behaviour. Until about 4 Gy, the dose response shows to be linear and then it becomes sublinear. None supralinearity appears between these two regimes. Saturation of the OSL signal is not observed because the maximal delivered dose was of 20 Gy and it is supposed to start above 50 Gy approximately.

However, the dose response curve presents a different behaviour when its data points are calculated using only part of the measured OSL signal. In this case, the dose response is initially linear, then it becomes supralinear and after this it starts the sublinear regimen.

At low doses the initial OSL intensity and the total OSL intensity are proportional to each other, but when dose increases, the initial intensity becomes supralinear. The point at which this occurs seems to depend on the integration time used in the calculation. In effect, when using integration times of few seconds (e. g. 6s) supralinearity starts earlier than when using longer times (e. g. 100s). However, if we continue increasing the integration time in Equation (6), we find a value at which the supralinearity is partially compensated by the sublinearity found for the total OSL intensity. Actually, when 700s were used in this test for the calculation of the initial intensity, a linear behaviour of the dose response with a coefficient of determination (R^2) of 0.9999 was observed until around 9 Gy (see Figure 5.4a, 700s). These observations suggest that when doing a calibration dose curve for a specific detector at a specific stimulation light power, one should look for the optimal integration time to be used for the calculation of the OSL intensity (not necessarily the total OSL intensity) so that the widest dose range of linear behaviour can be achieved for the used readout conditions. Now well, from this one can notice that the optimal integration time is not necessarily the total time used to estimate the total OSL intensity, nor a time involving only the peak of the OSL curve (first few seconds), but we do know that it may go up to several hundreds of seconds (for the experimental conditions used in this test) when the strong decay of the OSL signal has already occurred, but when the background level has not been reached yet. From this one should recognize that the linear behaviour intrinsic to the material itself is that one observed when using the total OSL intensity. However, as has been shown here, variants in the linearity of the OSL response can be obtained by tuning the integration time.

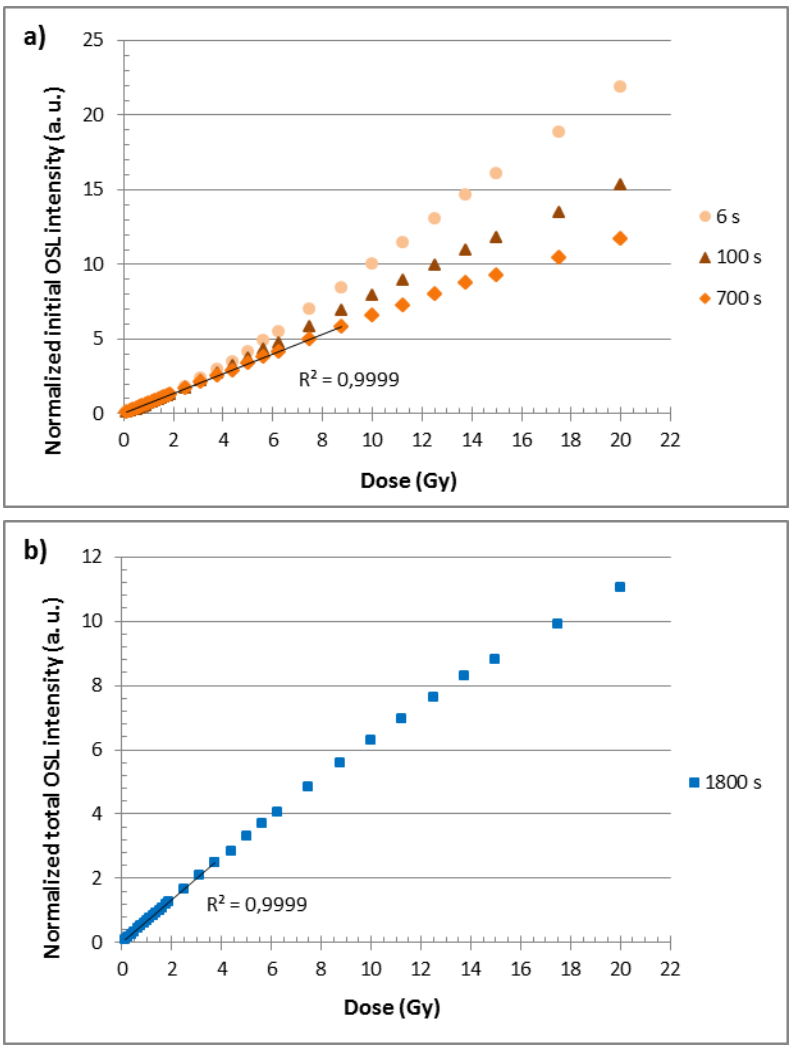

Figure 5.4. OSL response versus dose curves of beta of irradiated Luxel™ detectors using (a) initial OSL intensities and (b) the total OSL intensity. Each curve corresponds to the average of three detectors re-used several times, normalized to a dose of 1,5 Gy. Measurements were done using blue stimulation at 10% of the maximum power (~ 5 $mW.cm^{-2}$).

In general, supralinearity for Al_2O_3:C detectors has already been mentioned in other studies, but the dose at which it starts slightly varies from one work to another going from 1 Gy to about 3 Gy, maybe because different experimental procedures (which may include different integration times for calculations of the integrated OSL intensities) and forms of Al_2O_3:C detectors were used (Jursinic, 2007) (Miller, et al., 2008) (Reft, 2009) (Schembri, et al., 2007). However, any of the mentioned studies was done using blue instead of green stimulation and no remark was done about the dependence of the behaviour of the dose response curve on the choice of the stimulation time used to estimate the integrated OSL intensity. Differences in the dose response curve for the total and the initial OSL signals using green stimulation were commented by Yukihara *et al.*, but linear response was only achieved up to about 2 Gy, maybe because of the use of a short integration time (few seconds) (Yukihara, et al., 2004) (Yukihara, et al., 2011 p. 132).

Supralinearity in the initial OSL intensity dose response curve is related to the change of shape of the OSL decay curve when increasing the delivered dose. Figure 5.5 shows changes in the shape of the OSL curve of Luxel™ detectors depending on the delivered dose using beta particles. At doses lower than 1 Gy the shape of the OSL curve presents no changes, being almost the same. However, at higher doses, the OSL decay becomes more accentuated. This explains the supralinearity of Figure 5.4a for 6s and 100s. Having sharper OSL curves at high doses implies having higher initial OSL intensities. As high dose

effects in the shape of the OSL curve are stronger in the peak zone of it, initial OSL intensities at high doses calculated with short integration times deviate more from initial OSL intensities at low doses than those initial OSL intensities at high doses calculated with longer integration times, and therefore a higher supralinearity appears in the dose response chart when using only 6s than when using 100s or longer stimulation times.

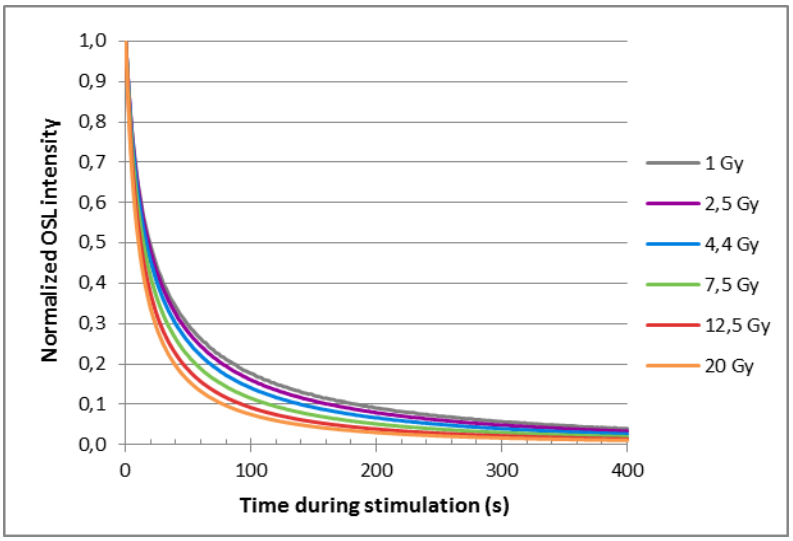

Figure 5.5. Changes in the shape of the OSL curve depending on the delivered dose. Each curve corresponds to the average of three detectors using blue stimulation at 10% of the maximum power (~ 5 $mW.cm^{-2}$) and the signal obtained was normalized.

Then, in order to get a better look of the degree of linearity of the OSL response over the absorbed dose, the linearity factor (*f(D)*) was calculated for each of the data points of Figure 5.4 (see Equation (7)). Calculations were done using as a reference of linearity the dose response obtained at 1,5 Gy.

As noted before, Figure 5.4a shows that points of test using 700s of integration time may be well approximated to the shown straight line with a coefficient of determination (R^2) of 0.9999 for the dose range between 0.126 Gy and 9 Gy. The same is observed for the total OSL intensity (Figure 5.4b), but only for the dose range between 0.126 Gy and about 4 Gy.

First statement is confirmed by the estimated linear factors. Figure 5.6-700s shows that the linear factor is approximately constant from the minimum dose until about 9 Gy, with a relative standard deviation of 0.7%. Then, for higher doses the dose response becomes sublinear and so the linearity factor starts decreasing. On the other hand, when the linear factor is calculated for the total OSL intensity data points, a slight level of sublinearity shows up for the minimum dose until about 0,5 Gy, revealing that a feeble sublinearity is also present in this dose range. Then, at higher doses the linear factor remains constant until about 4 Gy, when a decrease associated to a sublinear behaviour appears.

Both curves exhibit a sublinear behaviour at higher doses, but the degree of it for the same observed dose is different, being higher for the total OSL intensity. At 15 Gy the degree of sublinearity for the OSL intensity using 1800s is of 13.3%, whereas for the OSL intensity using 700s is of 7.9%, which means a 5,4% of difference. The same difference is observed at 20 Gy.

Regarding the OSL intensity calculated with the first 100s of stimulation time, Figure 5.6-100s confirms the high level of supralinearity as the linearity factor shows an increase of about 20% at 10 Gy. For doses above 14 Gy the linearity factor starts decreasing and the sub-linearity begins to appear.

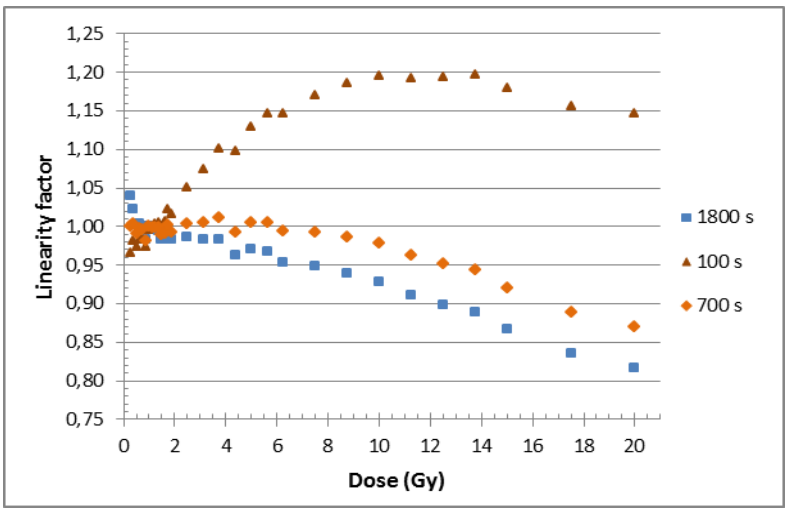

Figure 5.6. Linearity factor (*f(D)*) for the data points of the linearity test of Luxel detectors shown in Figure 5.4. Estimations were done using as a reference the dose response (OSL signal per unit of dose) obtained at 1,5 Gy.

The degree of tolerance of supra and sublinearity depends on the field of application in which the detector is used. For doses employed in diagnostic radiology a correction factor for nonlinearity effects of Luxel detectors can be considered unitary. However, in radiotherapy these effects should not be neglected and a correction factor must be accurately determined as higher doses are involved and measurements with high precision are needed. In accordance with this, a precise dose calibration curve from which the nonlinearity correction factor is estimated is also required.

5.1.2 Repeatability test

Thereafter, in order to account for the precision of the data obtained using the Risø OSL reader and Luxel detectors, repeatability tests for the readout of the OSL signal of a Luxel detector using the Risø system were performed and the associated relative standard deviations (RSD) were estimated.

For this, twelve consecutive sequences of bleaching/irradiation/OSL-stimulation steps over the same detector were carried out at two different stimulation light powers, using a test dose of 1,01 Gy of beta. Results for the normalized total integrated OSL intensities at 10% and 90% of the maximum stimulation light power (500s and 1800s as stimulation times respectively) are presented in Figure 5.7. At 90% the RSD was of 0.98% whereas at 10% it attained 1,4%. This is a predictable result since using low stimulation intensities implies measuring weaker OSL intensities, which means that there are less photons to be measured and higher uncertainties. However, both tests exhibited an unexpected behaviour in the values of subsequent measurements. The integrated OSL intensities show to decrease as measurements are done, with attenuations of up to 2,6% and 4,1% using the stimulation light at 90% and 10% respectively.

These effects can be caused by instabilities in stimulation or detection systems, related to a decrease in the sensitivity of the PMT while doing measurements, or to a decrease in the intensity of the blue light emitted by the set of LEDs but one should mention that this is very unlikely since the Risø reader has proved to be a reliable system for OSL measurements in innumerable studies. Besides this, a decrease in the sensitivity of the Luxel detector with the accumulated dose can produce the same effect observed in this test. No more tests were done to identify which was the specific cause of the decrease in the OSL signals, however, further tests should be done on this issue taking into account that this may represent another cause of an early sub-linearity in the dose response curve when successive OSL measurements are done in the Risø reader.

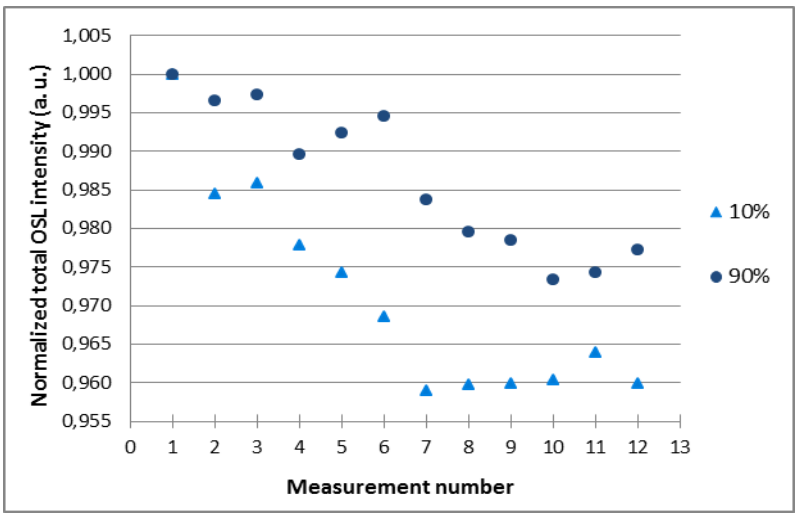

Figure 5.7. Reproducibility test of OSL measurements using the Risø reader at different stimulation light powers for a test dose of 1 Gy of beta particles.

5.1.3 Sensitivity test

Afterwards, another test intended to account for sensitivity variations as a function of the dose history of Luxel detectors was performed. As optical bleaching is not energetic enough to reach the deep traps of Al_2O_3:C crystals and release the charges trapped in these ones, previous irradiations of the detector have a cumulative effect in the filling of deep traps. The accumulated dose is estimated by adding all the previous doses received by the detector.

Figure 5.8 shows how the relative OSL sensitivity (see Equation (8)), defined as the OSL response following bleaching and irradiation with a fixed test dose, changes as a function of the dose previously accumulated by the dosimeters. For this, three new Luxel detectors which have never been irradiated before were used. The OSL sensitivity of the detectors for accumulated doses in the range from 0 Gy to 28,35 Gy of beta was obtained with a sequence of irradiations (D_i) and OSL readouts for the same detectors. After each OSL readout, detectors were bleached with blue light during 15 min. Then, the sensitivity of the samples was probed by delivering a test dose of 252 mGy and reading the resultant OSL signal. The procedure is summarized as follows:

1. Delivering of beta dose D_i;
2. Bleaching with blue light (100% of power) during 15 minutes;
3. Delivering of test dose of 252 mGy;
4. OSL readout during 1000s using blue light at 10% of the maximum power of the LEDs;
5. Bleaching with blue light (100%) during 15 minutes;
6. OSL readout for 60s at 10% to record the background.

This procedure was followed six times for each detector using different doses D_i: 0,63; 1,26; 2,52; 7,56 and 15,12 Gy in order to increase the accumulated dose of the detectors. Figure 5.8 shows the results for both total OSL intensity (t_f = 1000s) and three different peak intensities (t_p = 10, 100 and 500 s respectively). It can be seen that for the studied dose range, the OSL sensitivity increases when the detectors have received higher doses. When detectors have previously accumulated a dose of 28 Gy, the total OSL intensity shows to be almost 60% higher than when they have not been previously irradiated. However, when using the initial OSL intensity of the first 10s of stimulation, sensitization at 13 Gy is only of about 10% respect to the reference point and it seems to be constant until at least 28 Gy. Similarly, the background signal showed to increase with the accumulated dose too.

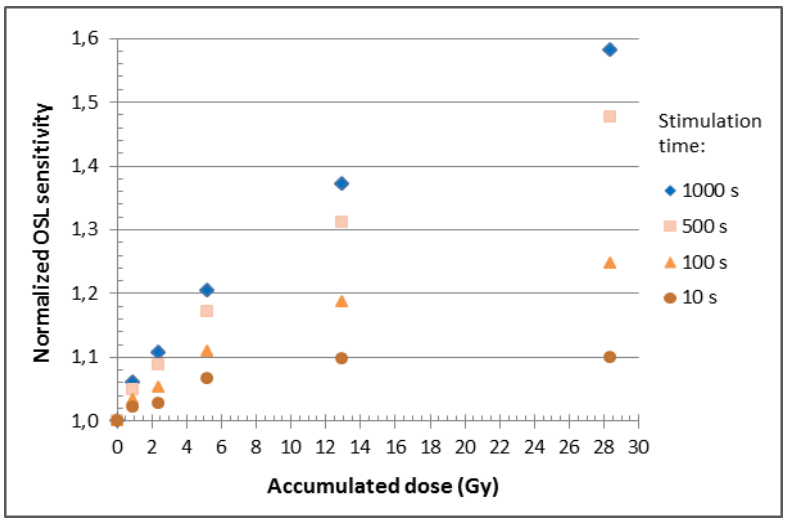

Figure 5.8. Relative OSL sensitivity of Luxel detectors following blue bleaching and beta irradiation with a fixed test dose of 252 mGy, as a function of the previous accumulated dose. Each point corresponds to the average of three detectors and are normalized to the OSL intensity obtained with the test dose (252 mGy).

Changes in sensitivity are related to a competition in the process of charge capture between different defects in the Al_2O_3:C crystals. In fact, competition between different trapping and recombination centers during either the irradiation or readout can cause the material to produce a higher OSL intensity that would be expected based on the response at low doses (sensitization). An example of such a process mentioned by Yukihara *et al*. that could lead to sensitization is the presence of deep trapping centers (Yukihara, et al., 2004). At low doses, the deep trapping centers compete for the capture of charges in the delocalized band during both irradiation and OSL readout. As a result, the OSL emission related to charges trapped at the main dosimetric trap is lower than would have been observed in the absence of deeps traps. Nevertheless, as the dose increases, deep traps become saturated, more charges are available for trapping at the main dosimetric trap during irradiation and less charges stimulated from the main dosimetric trap during readout are captured by the deep traps. The final result is that a more intense luminescence is produced than would be expected from the response at low doses, when deep traps are still empty.

In this sense, the increase in the OSL sensitivity when increasing the previous accumulated dose in Figure 5.8 indicates that filling of deep traps is occurring and therefore there is less competition for capture of charges in the delocalized band that can reduce the emission of luminescence. However, the degree of sensitization is not the same for the total OSL intensity as for the initial OSL intensity. Similarly as occurred in the dose response test, this difference is associated to a change in the OSL curve shape depending on the previous accumulated dose. Unlike Figure 5.5, at higher doses the OSL peak tends to be a little bit less sharp than as it would be at lower doses and therefore the initial OSL intensity increases. Moreover, the OSL signal at long stimulation times (e.g. > 20s) is superior at high previous doses, which in turns causes an increase in the total OSL intensity. These effects are illustrated in Figure 5.9. The OSL curves for 0,88 Gy and 2,4 Gy exhibit the mentioned differences respect to the curve obtained for 0 Gy (but slightly), which is in accordance with the increase of sensitivity observed in Figure 5.8.

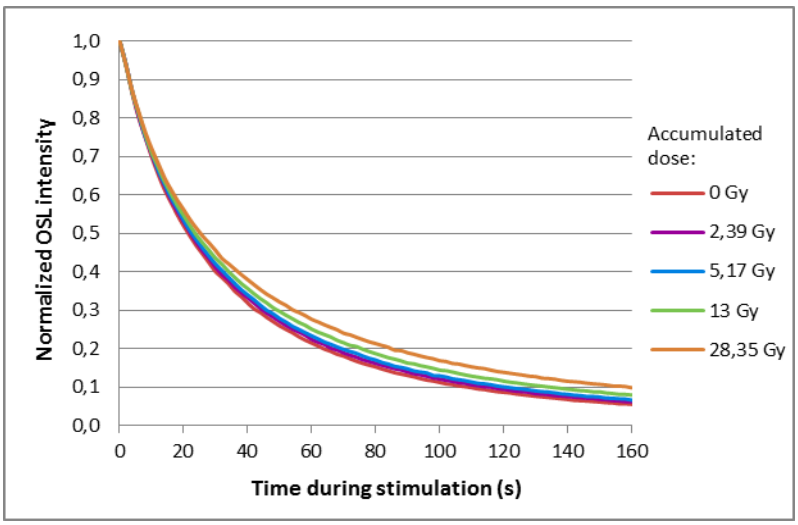

Figure 5.9. OSL curves of some of the data points of the sensitivity test shown in Figure 5.8. Each curve corresponds to the average of three Luxel detectors using blue stimulation at 10% of the LEDs power.

5.1.4 Fading test

Short-term fading of the OSL signal of Luxel detectors has already been reported by some authors (Jursinic, 2007) (Reft, 2009) (Yukihara, et al., 2010). Jursinic (2007) and Reft (2009) found a decrease of around 40% in the OSL signal of Luxel detectors, when it was measured about 10 minutes after irradiation with 1 Gy of 6MV x-rays, while Yukihara *et al.* (2010) observed a fading of 5% in beta irradiated ($^{90}Sr/^{90}Y$ source) Luxel detectors for the same period of time between irradiation and OSL readout. The three studies were done using green stimulation and fading estimations were done using initial OSL intensities with stimulation times of 1s.

Regarding long-term fading effects, Schembri *et al.* (2007) (Schembri, et al., 2007) and the authors mentioned before report fading rates smaller than 2% per day for the subsequent days after irradiation and even smaller and decreasing rates for longer periods of time depending on the study. However, long-term fading effects still have to be more thoroughly investigated since these observations do not agree with the results obtained by Yukihara and McKeever (2006) in a previous work, from which no significant fading effects were found for Al_2O_3:C detectors, but which was made using different experimental conditions (Yukihara, et al., 2006c).

At the moment, long-term fading effects are not strongly confirmed and seem to depend on the experimental conditions. Besides it, short term effects have been confirmed by several authors, but they have used only green light for the stimulation of the luminescence.

In this sense, some fading tests using blue stimulation were performed over beta irradiated Luxel detectors for different periods of time between irradiation and readout. Samples were irradiated with a dose of 1,26 Gy of beta particles and readout was performed lately with blue light at 90% of power (~ 45 $mW.cm^{-2}$). The detectors were re-used several times in order to perform the OSL readouts at different times after irradiation. Results for the first test are reported below in Figure 5.10.

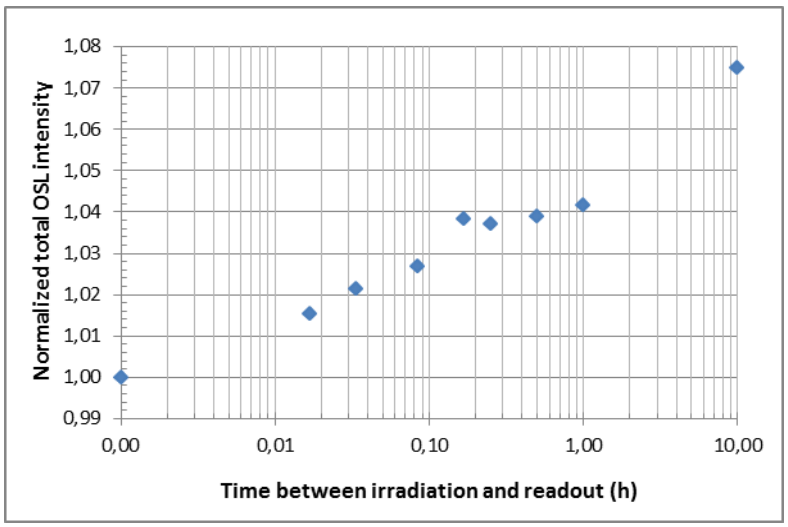

Figure 5.10. Fading test of a Luxel detector irradiated with 1,26 Gy of beta particles, kept inside the Risø samples chamber before readout of the OSL signal with blue light. Data points are normalized to the total OSL intensity measured just after irradiation (around 20s between irradiation and readout).

As illustrated in Figure 5.10, an abnormal behaviour of the OSL intensity over the elapsed time between irradiation and readout was found from this test. In fact, no fading was observed since the OSL intensity is not decreasing with the elapsed time. Instead of this, the total intensity is increasing at a rate that decreases with time (one should notice the logarithmic scale in the abscissa). After 1h the total integrated intensity is around 4% higher than when it is measured just after irradiation and after 10h it increases by almost 8%.

In other project developed at the RDC expert group of SCK•CEN, the presence of an intrusive x-ray field inside the Risø reader chamber was reported. This field seemed to be more intense in the sample position just below the $^{90}Sr/^{90}Y$ source, where it was measured to present a dose rate in air of 200 $\mu Gy.h^{-1}$. Supposing that a sample is placed below the beta source, for a period of time between irradiation and readout of 10h the delivered x-ray dose to the sample would be of 20 mGy. Based on a linear behaviour of the dose response of the detector used for the test shown in Figure 5.10, an increase of 20 mGy in its dose would mean an increase of 1,6% in the OSL observed after 10h. However, as mentioned before the increase at that point is of ~ 8%, so there is still a 6% of signal with unknown provenance, assuming that the detector does not present fading effects.

Nevertheless, in order to discard any probability of an additional irradiation of detectors during the time between irradiations and OSL readouts that may increase the OSL response of detectors, several fading tests were repeated taking the detectors out of the chamber of the reader and putting them in a dark case during the period of time before the OSL readout. Unfortunately, the obtained results exhibited a high dispersion and any preferential behaviour was observed among all tests and therefore they are not shown here.

In this way, the repeatability of the OSL measurements using the Risø reader was again assessed over a Luxel detector. Measurements were done using the blue light at 90% of the maximum power and a fixed dose of 1 Gy. Between each bleaching/irradiation/readout sequence the samples chamber of the reader was opened and exposed to the room light (a weak red bulb) and the detector was taken out for 3 minutes before the next measurement was done. The relative standard deviation obtained for the total OSL intensity for 12 repeated measurements showed to be high reaching a value of almost 9%. This high variability in the OSL results may suggest the presence of instabilities in the reader system that must be thoroughly checked up in order to account for the precision of the OSL measurements. Another source of variability is related to the position of the detector in the sample holder since this one is

changing between measurements and that can introduce some alterations during the detection of the OSL signal. However, as the fading test was one of the last experiments performed during this project, there was not enough time to clarify the cause of this variability, but this is something that will be done further on.

Despite the inconvenience to perform the fading test taking the detectors out of the reader, it is still important to remark that a similar phenomenon as the illustrated in Figure 5.10 has been observed by Jursinic (2010) when he was studying the changes in the dosimetric properties of OSLDs with the accumulated dose (Jursinic, 2010). His work reports an increase in the OSL signal of bleached detectors who were stored in the dark that is proportional to the previous dose received by the detectors. The regenerated signal in about 4 days is equivalent to 220 mGy for bleached detectors with an accumulated dose of 180 Gy of 6 MV x-rays and of about 100 mGy for detectors with an accumulated dose of 120 Gy. For the last ones, the regenerated signal after 10 hours is near 20 mGy.

As the dose history of the detectors used in these tests is not well known, it is possible that a similar effect as that observed by Jursinic is occurring in Figure 5.10, but with irradiated samples instead of bleached ones. An explanation of this phenomenon can be found in his work (Jursinic, 2010). Additional experiments with previously irradiated and new detectors should be done to evaluate whether a similar phenomenon may be causing the increase in the OSL signal of Luxel detectors.

5.1.5 Linearity test using ^{60}Co-gamma rays

The OSL response of Luxel detectors to ^{60}Co gamma rays was assessed by means of a linearity test. Different sets of 4 detectors were irradiated with a specific dose in the range of 100 mGy to 60 Gy.

To avoid saturation of the PMT at such as high doses blue light was used only at 1% of the maximum power (~ 0,5 mW.cm^{-2}). The results for the integrated OSL intensity obtained at 2000s of stimulation time are shown in Figure 5.11.

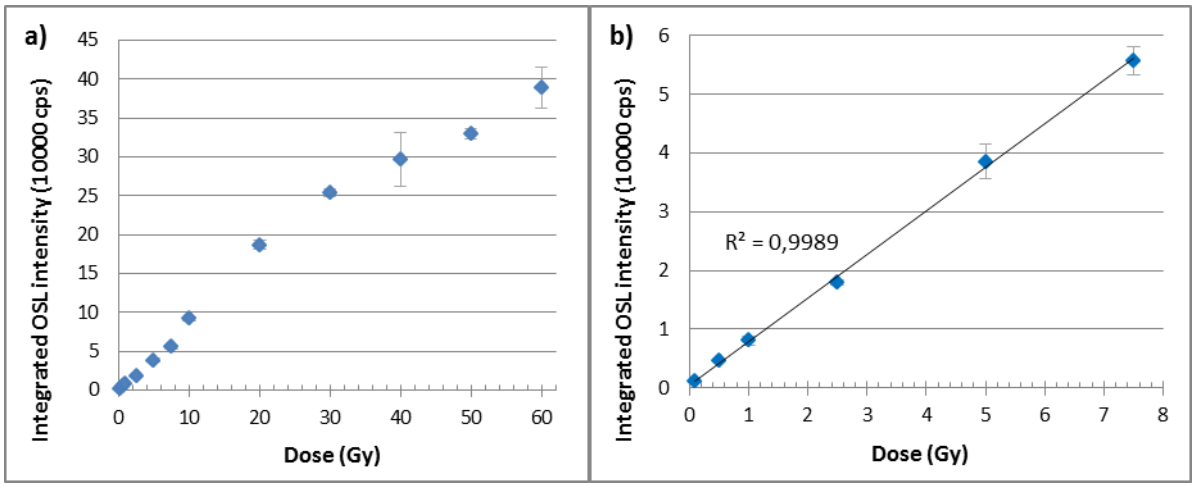

Figure 5.11. OSL response versus dose curve of Luxel detectors using ^{60}Co gamma rays and blue stimulation at 1% (~ 0.5 mW.cm^{-2}). Each point corresponds to the average of the integrated OSL intensities of four detectors with their respective standard deviation (error bar). Figure (b) presents the data points for doses below 7,5 Gy from figure (a).

Data points in Figure 5.11 present high dispersion and do not behave as well as those obtained with beta particles. This is to some extent expectable considering that each data point represents a different set of 4 detectors, a much lower stimulation light intensity was used and OSL measurements were done at different times, with detectors that were not irradiated inside the Risø, but by another laboratory of SCK•CEN (KAL).

Because of the mentioned reasons and the poor number of data points, performing a precise assessment of the quality of this linearity is not really possible. However, looking to the range between 100 mGy and 7,5 Gy (Figure 5.11b) one can say that the OSL response to gamma photons shows a linear behaviour. Then, above 7,5 Gy a supralinear regime seems to appear until about 40 Gy, from where the OSL signal starts saturating. This supralinear behaviour is consistent with changes in the OSL decay curve that were observed when increasing the absorbed dose, as occurred in the linearity test of beta irradiated Luxel detectors.

5.2 Measurements using powder detectors

As mentioned in section 4.1.1.3, powder samples were prepared using a photo-curable polymer as matrix to hold the powder. In order to evaluate whether the polymer was appropriate to be used in powder samples, some tests with drops of hardened polymer (without powder) were previously performed.

First, the background signal of several non-irradiated polymer samples obtained when they were illuminated with blue light at 100% (~ 50 $mW.cm^{-2}$) was measured. Then, samples were irradiated with different beta doses from 100 mGy to 100 Gy to see whether they were OSL sensitive to ionizing radiation or whether their physical appearance changed with it. The same was followed with drops of different volumes of polymer. Later, after these tests, more polymer samples were prepared but using different times of exposure to the UV source in order to evaluate whether the curing time had some influence in the luminescent behaviour of the polymer. In all cases, sample holders of the Risø reader had to be well cleaned before they were used to remove any possible Al_2O_3:C powder particles from other kinds of powder samples tested before.

The obtained results for all tests showed that the OSL signal of powder samples is always a background level between 200 and 400 counts per second (cps). This level is comparable to 200 cps, which is the signal measured from an empty sample holder at the same stimulation light power. The polymer did not show to be sensitive to ionizing radiation, nor it showed any OSL response. Its aspect did not changed and the background level did not increase when drops of higher volumes were used.

5.2.1 Powder concentration test using $^{90}Sr/^{90}Y$ beta particles

The first test using powder samples sought to determine the minimum amount of powder necessary to perform a dosimetric measurement with the Risø reader. Knowing this value can be interesting in dosimetry considering that the less amount of powder used per dosimeter, the less is the perturbation caused by the detector in the radiation field that is irradiating the place where the measurement takes place (e.g. human tissue). Also, a direct consequence is that the less the amount of powder, the smaller the size at which the detector can be made and therefore higher the spatial resolution of it.

In this way, samples of different powder concentrations were prepared following the protocol described in section 4.1.1.3. The lower limit volume of the micro-pipette was 1 μl, so all polymer samples were prepared using this volume of powder solutions (polymer + Al_2O_3:C powder) to reduce the size of detectors and thus to improve their spatial resolution. To assess the OSL response of powder detectors a fixed dose of 1,26 Gy of beta particles was used. Readout was done during 60s of stimulation with blue light at 100% (~ 50 $mW.cm^{-2}$). The OSL curves of samples with different concentrations of powder are shown in Figure 5.12.

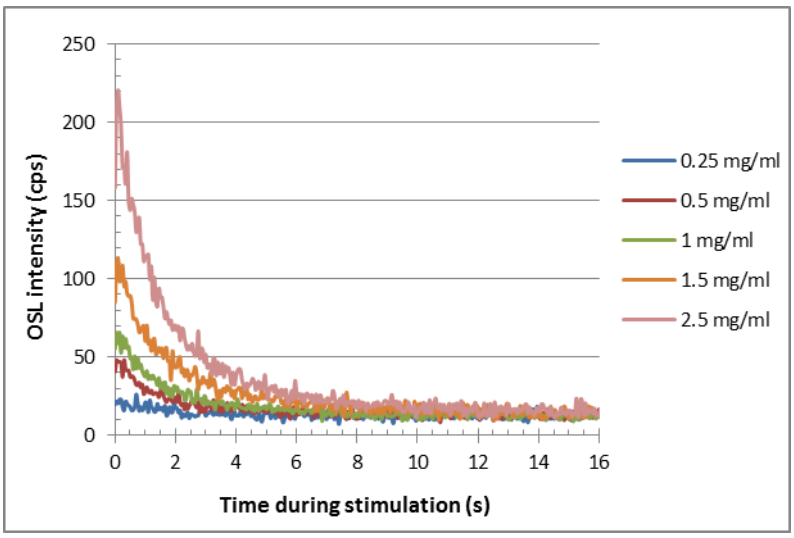

Figure 5.12. OSL curves of 1 µl samples with different concentration of Al_2O_3:C powder who were irradiated with 1,26 Gy of beta particles. Each curve corresponds to the average of four samples. Measurements were done using the Risø reader with blue stimulation light at 100% (~ 50 $mW.cm^{-2}$).

It can be seen that when the amount of powder per sample increases, the OSL signal does it either. As there are more Al_2O_3:C particles (crystals) in the detector, the number of radiative centers available to trap excited charge carriers is higher. Thus, when irradiating the detector, a higher portion of the charge carriers formed by the electron collisions (both the initial beta beam and secondary electrons) get trapped in these centers. Later, when stimulation with light is performed, as more full traps are emptied, more photons are emitted from their subsequent relaxation and the detected luminescence is more intense. This dependence can be better observed in Figure 5.13, where the weighted total OSL intensity of detectors (total OSL intensity of each detector divided by its weight) is plotted against the concentration of powder.

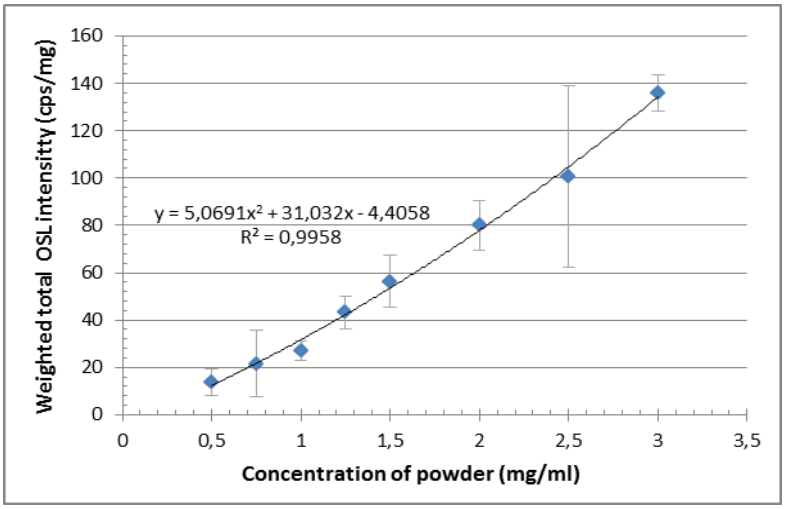

Figure 5.13. Total integrated OSL intensity of 1 µl samples with different concentration of powder who were irradiated with 1,26 Gy of beta particles. Measurements were done using the Risø reader with stimulation light at 100% (~ 50 $mW.cm^{-2}$). Each data point corresponds to the average of 3-5 detectors with their relative standard deviation (error bar). The total OSL intensity of each detector was divided by its weight to reduce the dispersion of detectors with same concentration of powder.

Regarding the minimum amount of powder detectable with the Risø, one can see in Figure 5.12 that samples prepared with solution of 0,25 mg/ml (25 µg of powder per detector) do not show an OSL peak during stimulation. The poor number of charges that got trapped in these samples was not sufficient to

generate a luminescence intense enough to be well detected by the PMT and so the OSL intensity was too weak and no peak was observed.

As mentioned in section 3.1.1, the lower dose limit of a dosimeter may be defined to be the dose necessary to double the instrumental background reading (Attix, 1986 p. 279). Similarly, for a given absorbed dose, one can say that the minimum concentration of powder necessary to have a useful powder detector is that one required to double (at least) the background signal of the detector. As shown in Figure 5.12, samples of 0.25 μg do not meet this requirement since the maximum value of the averaged OSL signal in Figure 5.12 is just 50% higher than the background level. However, samples with 0.5 μg present a small but visible peak in the averaged OSL signal. The height of the peak is about 3.6 times the value of the background signal (i. g. ~ 260% higher). Now, one can say that the minimum amount of powder needed to detect a dose of 1,26 Gy of beta particles in 1 μl polymer detectors is of around 0,5 μg.

However, this amount of powder is useful only if doses equal to or higher than 1,26 Gy of beta are going to be used (measured in the practice). If a lower dose is to be measured, more powder is needed so that the OSL can be detected by the PMT. From another test that will be shown later in section 5.2.3, it was found that a 1 μl sample with 10 μg of powder is capable of detecting a dose of 126 mGy, that was the minimum dose that could be delivered with the $^{90}Sr/^{90}Y$ source of the Risø at that moment.

Something important to be pointed out here is that the OSL intensities measured from samples that were supposed to be equal (i. g. prepared with the same protocol and using the same amount of powder and polymer) in several cases presented high dispersion (see the error bars in Figure 5.13). Differences between results of similar samples may be mainly associated to experimental errors during samples preparation as e. g. when measuring volumes of solution slightly different with the micro-pipette, causing an excess or a deficiency in the amount of powder per sample and thus an increase or decrease in its OSL intensity. With respect to this, a particular test was done to have an idea of how different were the volumes of samples that were supposed to be of 1 μl. Using a powder solution of 0.7 mg/ml, 20 samples of 1 μl were prepared using the same protocol and solution. After curing them with UV-light, the detectors were weighted in a high precision balance (standard deviation of 0,02 mg). If all the samples are of 1 μl, then their weights should be the same for all of them. However, since the dispersion obtained from the measured masses was of about 8%, one can deduce that the detectors presented an important variability in its volume and therefore in the quantity of powder. This was the reason for which the OSL intensities in Figure 5.13 were divided by the mass of the detectors.

Some other sources of error that are possibly causing the high dispersion of the results in Figure 5.13 are those related to (i) the uncertainty of the OSL measurements when detecting luminescence of low intensity, (ii) the inhomogeneities of the dispersion of the powder in polymer solutions and (iii) the variability of sensitivity of powder grains between one sample and other.

5.2.2 Powder concentration test using ^{60}Co gamma rays

The same samples used for the powder concentration test with beta particles in the last section were also tested using ^{60}Co gamma photons. Samples were bleached with blue light in the Risø reader, then irradiated with 1,26 Gy of gamma rays in another laboratory and later after few hours (unknown with exactitude) they were read in the Risø reader with blue light at 100% of power. Figure 5.14 illustrates the obtained results for the weighted total OSL intensities.

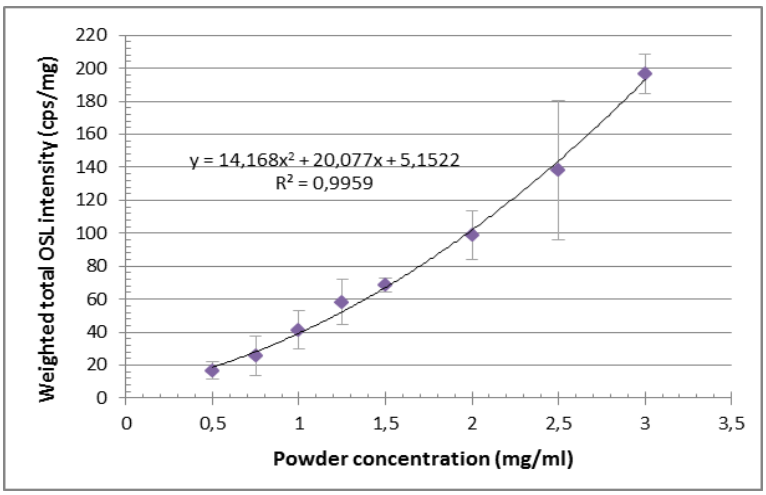

Figure 5.14. Total integrated OSL intensity of 1 µl samples with different concentration of powder who were irradiated with 1,26 Gy of gamma rays. The same samples of Figure 5.13 and the same experimental conditions were used in these measurements, but samples were irradiated with ^{60}Co gamma rays instead of beta particles.

In comparison with the results obtained when irradiating with beta particles (see Figure 5.13), the OSL response of powder detectors is higher when using the same dose of ^{60}Co gamma rays. The total OSL intensities of powder detectors for gamma photons are between 20% and 50% higher than for beta particles. At 3 µg of powder, e.g., the integrated intensity in Figure 5.14 is 1,45 times the value in Figure 5.13. This behaviour may be an effect of the short range of beta particles compared to the high penetrating power of gamma photons when passing through matter. As uncharged particles have more probabilities than charged particles of passing straight through matter without losing energy (due to absence of electrical charge), for comparable energies, uncharged particles tend to penetrate much farther through matter than charged particles. In this case, a considerable number of electrons from the ^{90}Sr/^{90}Y source may be stopped by the polymer before reaching the powder particles. Now, as there are less beta particles interacting with the micro crystals of Al_2O_3:C, less electron-hole pairs are produced and then less luminescence is released when stimulating with light. Other case may be that in which beta particles interact with the powder, but lose their energy so fast that then they are not able to reach farther particles or cannot ionize those that they reach. This assertion has to be confirmed by studying the interaction of beta and gamma with a mixed medium of water equivalent medium (like this polymer) and Al_2O_3:C particles. However, as a reference one can mention that the CSDA range for beta particles of 2,27 MeV in a water equivalent medium is around 1 cm, while the inverse of the coefficient of absorption (distance needed to decrease by 63% the intensity of a ray while passing through a medium) of an X-ray (similar nature to that of gamma) of 1,25 MeV in water is around 15 cm.

This effect might be one reason to explain why the OSL response of prepared powder detectors is different for gamma rays than for beta particles. Besides this, there is also the fact that the absorbed dose in a material depends on the energy of the incident radiation. In a simple model, the absorbed dose is proportional to the energy absorption coefficient of the material (Yukihara, et al., 2011 p. 123). This coefficient depends on the atomic number of the material and on the energy of the incident radiation. In our case two radiation fields with different energies were used and it is known that Al_2O_3:C is energy dependent.

However, as the detectors were previously irradiated with beta (to perform the test of section 5.2.1) and then bleached, possible accumulated dose effects like changes in sensitivity should also be taken into account to see how much each effect may be contributing with the observed behaviour of the detectors and then, know how much different is the OSL response of the detectors to one field compared to another one.

5.2.3 Linearity test using $^{90}Sr/^{90}Y$ beta particles

First linearity test of powder detectors was performed using 1 µl samples with 1 µg of powder. A set of four detectors was bleached with blue light in the Risø reader, irradiated with doses between 126 mGy and 15,12 Gy of beta particles and then stimulated with blue light at 100% of power (~ 50 mW.cm^{-2}). Detectors were not new but the specific dose history is not known. The dose response curve for the total OSL intensity (t_p = 60s) from 1,13 Gy is shown in Figure 5.15.

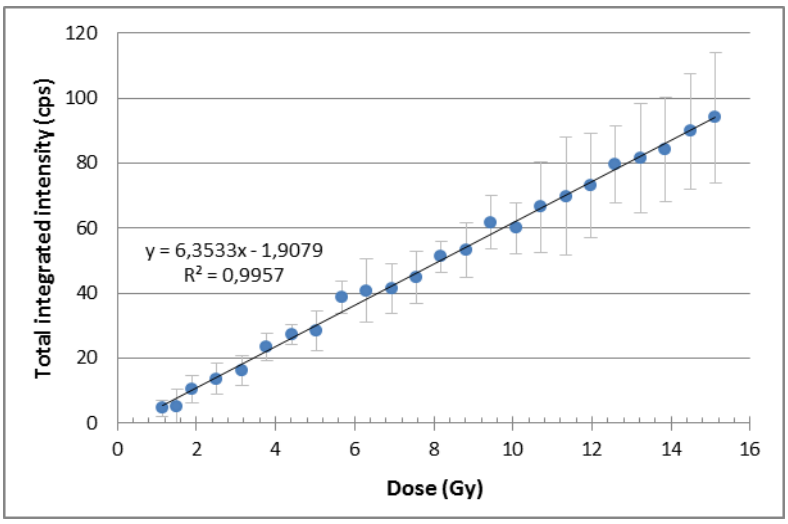

Figure 5.15. OSL response versus dose curve of 1 µl powder samples with 1 µg of powder using beta particles and blue stimulation light at 100% of power (~ 50 mW.cm^{-2}). Each data point corresponds to the average of the total OSL intensities (t_f = 60 s) of four re-used detectors and their associated standard deviation (error bar).

The figure above shows that the total OSL response of detectors of 1 µl with 1 µg is linear for the dose range between ~ 1,1 Gy (the lower limit to detect the OSL signal for this amount of powder, using the Risø) and 15 Gy. The small amount of powder used per sample increases the uncertainty of the OSL measurements. Nevertheless, we can see the linear behaviour of the results.

Then, in order to have more precise measurements of the dose response curve of powder detectors and to be able to use lower beta doses, four samples of 1 µl with 10 µg of powder were prepared and the same test was repeated using beta doses from 126 mGy to 15,12 Gy. An important difference in this test is that samples were new, which means that they had never been irradiated before. The results for both the total and the initial OSL intensities (t_f = 60s and t_p = 1s respectively) are shown in Figure 5.16.

As occurred with Luxel detectors, the behaviour of the dose response depends on the integration time used to estimate the integrated OSL intensity. However, from Figure 5.16 one can see that the dose response for the initial and the total OSL intensities present a sublinear behaviour all over the tested dose range and any linear behaviour is seen even at low doses. Unlike Luxel detectors, the initial and the total OSL intensities are proportional to each other until about almost 4 Gy. This is corroborated when the normalized OSL decay curves are plotted within the same graph so that changes in shape can be observed. Between 0.63 Gy and 3.8 Gy the OSL curve has a similar shape, but at higher doses the OSL peak becomes sharper, as observed for Luxel detectors. This effect can be regarded in Figure 5.17.

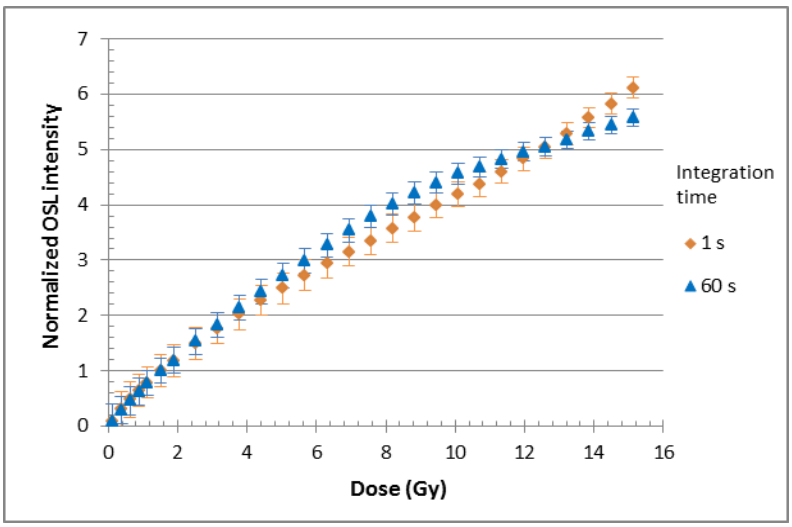

Figure 5.16. OSL response versus dose curve of 1 µl powder detectors with 10 µg of powder irradiated with beta, using blue stimulation light at 100% of power (~ 50 mW.cm^{-2}). Each data point corresponds to the average OSL intensity of four re-used detectors and their percentage standard deviation (error bar) Data points were normalized to the OSL intensity at 1,51 Gy.

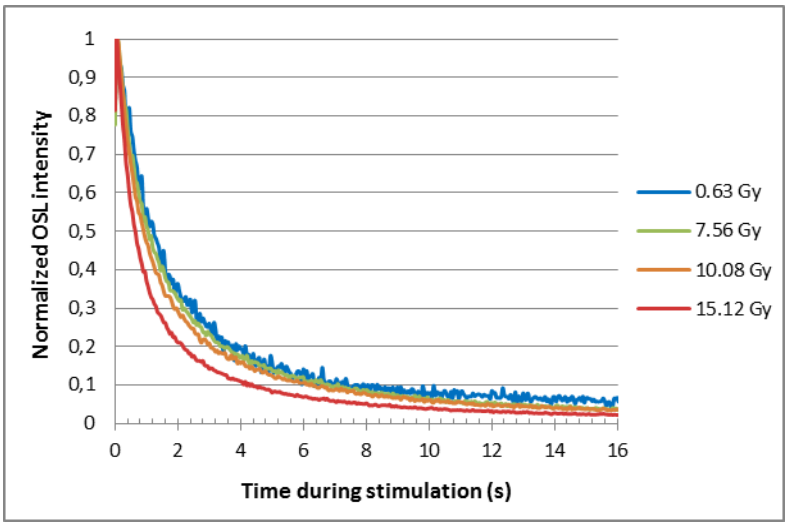

Figure 5.17. Changes in shape of the OSL curves of 10 µg powder detectors irradiated with different doses of beta particles. Each curve corresponds to the average of four detectors re-used for each dose.

Then, this test was repeated with the same four samples of 10 µg used in the test before to see whether it occurred a change in the dose response of powder detectors depending on the dose history of them. Adding all the delivered doses used for the test of Figure 5.16, an accumulated dose of 192 Gy is obtained for these detectors (for the first point of the next figure). The results for the total OSL intensity and the initial OSL intensity at the optimum time are presented in Figure 5.18.

In contrast to what was observed in Figure 5.16, the OSL response of detectors with an accumulated dose higher than 192 Gy is linear until about 10 Gy when using the appropriate integration time for the estimation of the initial OSL intensity. Using the Total OSL intensity, a linear behaviour is seen up to about 6,3 Gy with a coefficient of determination (R^2) of 0,9999 for the linear approximation. This is confirmed in Figure 5.19 were the linearity factor is plotted against the absorbed dose. One can say that the initial OSL intensity is linear until about 10 Gy considering a variation of 5% in the linearity factor. However, main variation is seen at low doses for both the initial and the total OSL intensities, which suggests that it may be related to the higher uncertainty of the measurements at these doses due to the low intensities of the luminescence.

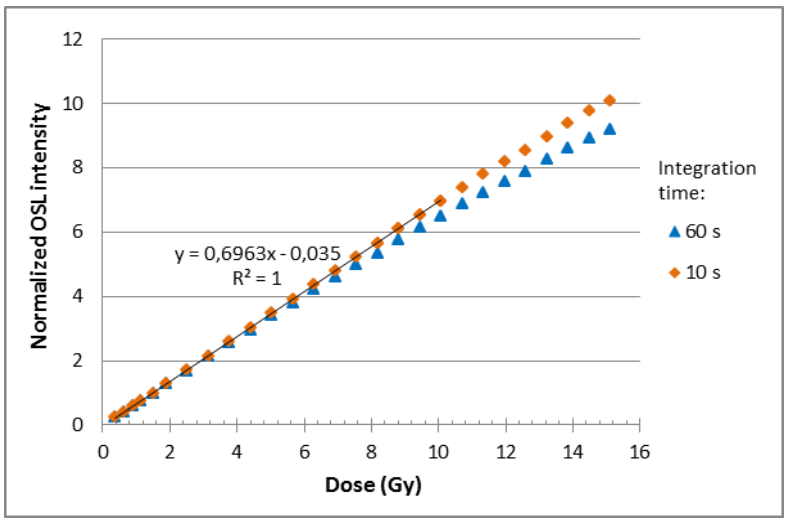

Figure 5.18. Repetition of the linearity test in Figure 5.16 using the same samples (detectors of 1 µl with 10 µg of powder) with an accumulated dose of 192 Gy of beta. Each data point corresponds to the average OSL intensity of the set of four detectors. Data points were normalized to the OSL intensity at 1,51 Gy.

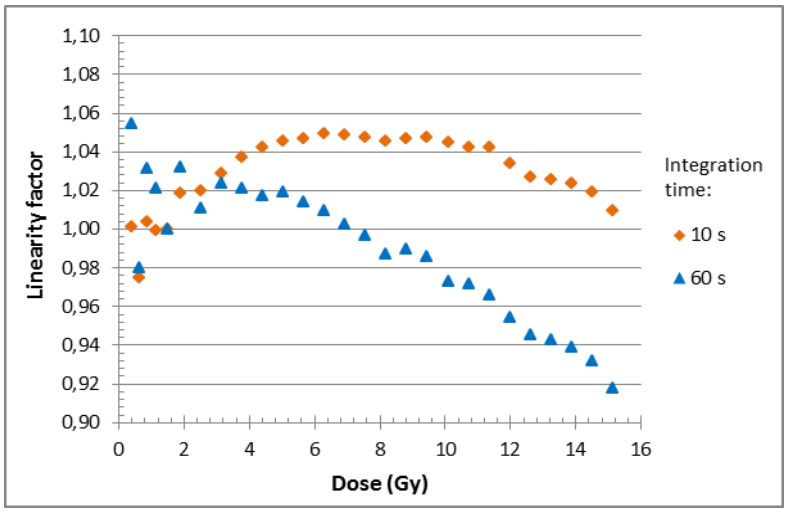

Figure 5.19. Linearity factor (*f(D)*) for data points of the linearity test of powder samples presented in Figure 5.18. Estimations were done using as a reference the dose response obtained at 1,51 Gy.

The change in the behaviour of the dose response curve observed in Figure 5.18 indicates that the sensitivity of powder detectors is varying within the accumulated dose. In effect, comparing the total OSL intensity obtained at an absorbed dose of 0.63 Gy for both tests (same tests in Figure 5.16 and Figure 5.18, but without normalizing the OSL intensities) it was seen that when the detectors presented an accumulated dose of 192,3 Gy (accumulated dose until data point of 0.63 Gy of absorbed dose in the test of Figure 5.18) the total OSL intensity was about 50% lower than that one obtained for 0.63 Gy in Figure 5.16, where the detectors possessed an accumulated dose of just 0,5 Gy (due to the lower irradiations of the same linearity test). In addition, when comparing the total OSL intensities obtained at 10 Gy, it was observed that the difference between both results decreased, being about 25% less the OSL intensity obtained at an accumulated dose of 280 Gy (accumulated dose until data point of 10 Gy of absorbed dose in the test of Figure 5.18) than that one obtained at an accumulated dose of 88 Gy, for the same point of the test in Figure 5.16. Another test accounting for changes in sensitivity within accumulated dose will be done in future work in order to see whether there is an accumulated dose above which these changes stop appearing.

5.2.4 Sensitivity test

Changes in the sensitivity of powder detectors were tested for accumulated doses between 0 Gy and 22 Gy of beta particles. After each increase of the accumulated dose, detectors were bleached with blue light, irradiated with a test dose of 252 mGy of beta and then the resultant OSL signal was measured. Changes in this OSL were followed for five different accumulated doses up to 22 Gy. Figure 5.20 shows the results for both the total OSL intensity (t_f = 60s) and a peak intensity with t_p = 1s obtained when stimulating with blue light at the maximum power (~ 50 mW.cm^{-2}).

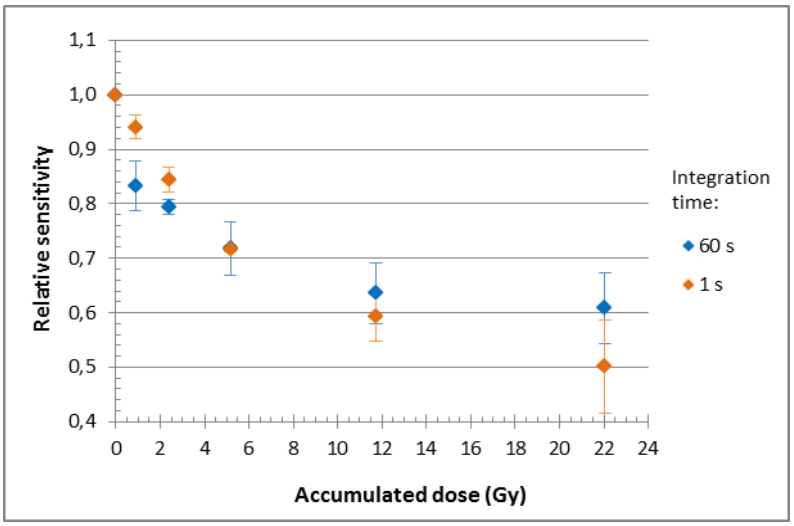

Figure 5.20. Relative OSL sensitivity of new detectors of 1 µl with 10 µg of powder following blue bleaching and beta irradiation with a fixed test dose of 252 mGy, as a function of the accumulated dose. Each point corresponds to the average of three detectors and their associated standard deviation. Values are normalized to the OSL intensity obtained at 252 mGy.

Unlike Luxel detectors, in Figure 5.20 it can be seen that the OSL sensitivity of powder detectors decreases when increasing the accumulated dose for the studied accumulated dose range. When detectors have an accumulated dose of 22 Gy of beta, the total OSL intensity shows to be about 60% of the total intensity that when they have not accumulated any previous dose (0 Gy). This effect is stronger in the initial OSL intensity, for which the sensitivity decreases by about 50% for the same accumulated dose. However, according to the behaviour of the group of data points, the relative OSL sensitivity seems to stabilize at higher accumulated doses and it seems to happen firstly in the total OSL intensity.

In future work higher accumulated doses between 20 Gy and 400 Gy should be tested for powder samples so that a correlation with the results obtained from the linearity tests in Figure 5.18 can be done. Also, another test with accumulated doses over 400 Gy is needed in order to investigate whether the sensitivity of detectors stabilizes at higher accumulated doses. Finally, if this is the case, then it would be possible to perform a repeatability test of the OSL measurements in the Risø reader by giving a high pre-dose to the samples to stabilize them and avoid changes in the OSL results due to changes in sensitivity of the detectors.

5.2.5 Linearity test using ^{60}Co gamma rays

The dose response of powder detectors to gamma photons was investigated using six samples of 1 µg of Al_2O_3:C powder. First, samples were bleached with blue light in the Risø reader, then they were irradiated with gamma rays in the KAL laboratory and later they were read in the Risø reader with blue light at 100% of power (~ 50 mW.cm^{-2}). The same set of samples was used for all tested doses, between 100 mGy and 10 Gy. Figure 5.21 illustrates the results for the total OSL intensities using a stimulation time of 60s.

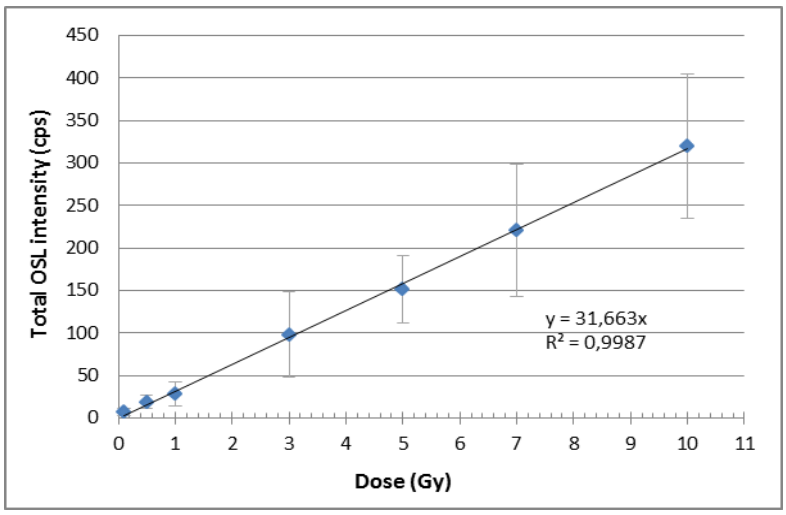

Figure 5.21. OSL response versus dose curve of 1 µl powder samples with 1 µg of powder using gamma rays and blue stimulation light at 100% of power (~ 50 mW.cm^{-2}). Each data point corresponds to the average of the total OSL intensities (t_f = 60s) of six re-used detectors and their associated standard deviation (error bar).

As well as it was commented in the concentration test using gamma photons (section 5.2.2) and as it can be seen in this test, powder detectors exhibit a higher OSL response to gamma photons than to beta particles since the measured OSL intensities are higher when irradiating with gamma than with beta rays. Also, despite of the already mentioned dispersion that is observed for tests with gamma, Figure 5.21 shows that the dose response of powder samples is linear for the tested gamma dose range.

In a future work, performing a sensitivity test using gamma rays would be interesting once the response of the detectors is different for these two types of radiation (beta and gamma).

5.2.6 Fading test

The last test presented here for powder detectors is the fading test. As it was done with Luxel detectors, the stability of the OSL signal over the time between irradiation and readout was investigated for samples with 10 µg of powder. The detectors were irradiated with a dose of 1,26 Gy of beta particles and the readout was performed with blue light at 100% of power (~ 50 mW.cm^{-2}). The samples were re-used several times in order to perform the OSL readouts at different times after irradiation. The results are reported in Figure 5.22.

The same abnormal behaviour observed for Luxel detectors is seen for powder detectors in Figure 5.22. The OSL signal, instead of being stable or showing a fading effect is increasing over the time elapsed after irradiation. For a period of 70 minutes after irradiation, the signal is between 7 and 12 % higher respect to the OSL signal obtained just after irradiation, while for a period of three days it presents an increase of 15-30% depending on the detector.

This test was repeated taking the samples out of the reader between irradiations and readouts but the obtained results also presented high dispersion and any preferential behaviour was observed. A discussion about this was done in section 5.1.4.

Until now the causes of this behaviour are not known, nevertheless, in order to perform this test in better conditions the stability of the OSL measurement in the Risø reader and the stability of the sensitivity of detectors within irradiations must be first assured so that other phenomena are not involved in the obtained results. Also, other bleaching procedures can be tested (e.g. bleaching with white day light) in order to investigate whether the type of bleaching has some influence in the behaviour observed in Figure 5.22.

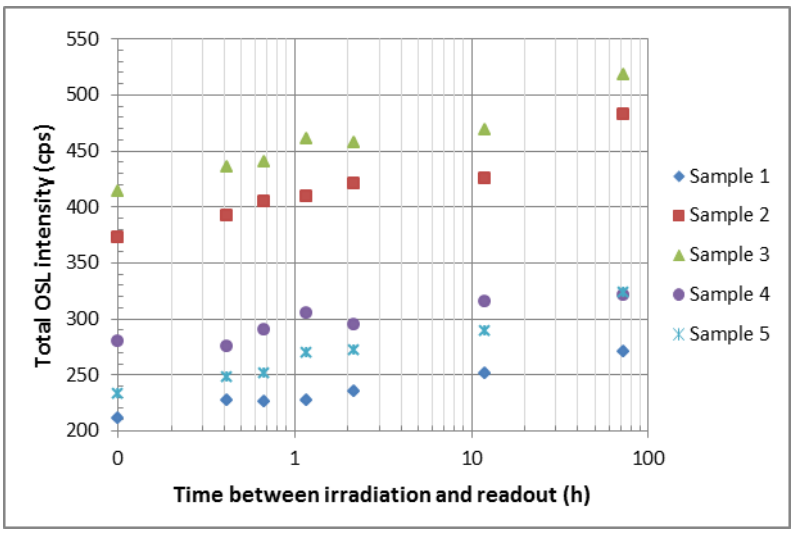

Figure 5.22. Fading test of five powder detectors of 10 µg irradiated with 1,26 Gy of beta particles, kept inside the Risø samples chamber before readout of the OSL signal with blue light.

5.3 Measurements using the single crystal

As mentioned before, measurements using the Al_2O_3:C single crystal were more limited because only one detector was available. For comparison with powder and Luxel detectors, the linearity test for beta particles is shown below.

5.3.1 Linearity test using $^{90}Sr/^{90}Y$ beta particles

The dose response of the single crystal to beta particles was assessed for doses between 126 mGy and 12,6 Gy using the Risø reader. After each irradiation, the single crystal was stimulated with blue light at 3% of the maximum power during 2000 seconds. Bleaching steps were done inside the reader using blue light at 100% during about 15 minutes to clear the residual signal of the detector. Figure 5.23. illustrates the results for the integrated OSL intensity using a stimulation time of 2000s.

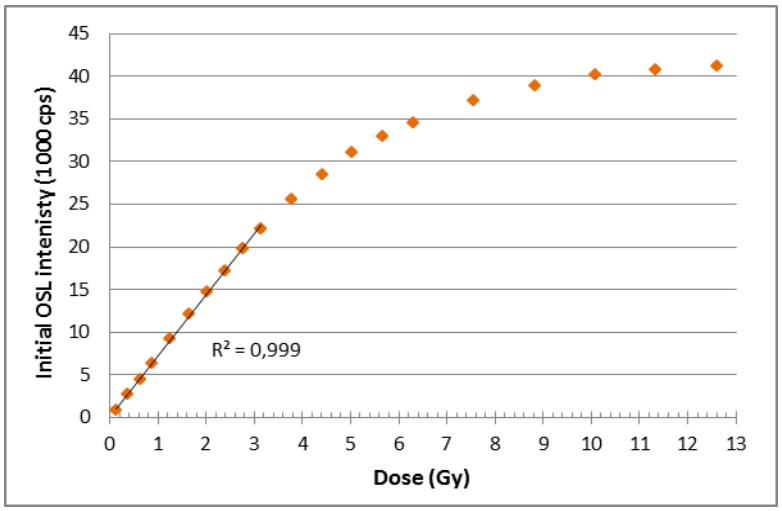

Figure 5.23. OSL response versus dose curve of the Al2O3:C single crystal irradiated with beta particles and using blue stimulation light at 3% of power (~ 1,5 mW.cm-2).

In Figure 5.23 one can see that the OSL response of the single crystal to beta particles is approximately linear only up to about 3 Gy (coefficient of determination of 0.9990). For higher doses it starts a saturation behaviour and then above 10 Gy the sensitivity tends to zero and the beginning of a plateau in the dose response is observed. The degree of linearity of the dose response in Figure 5.23. can be better observed in the figure below.

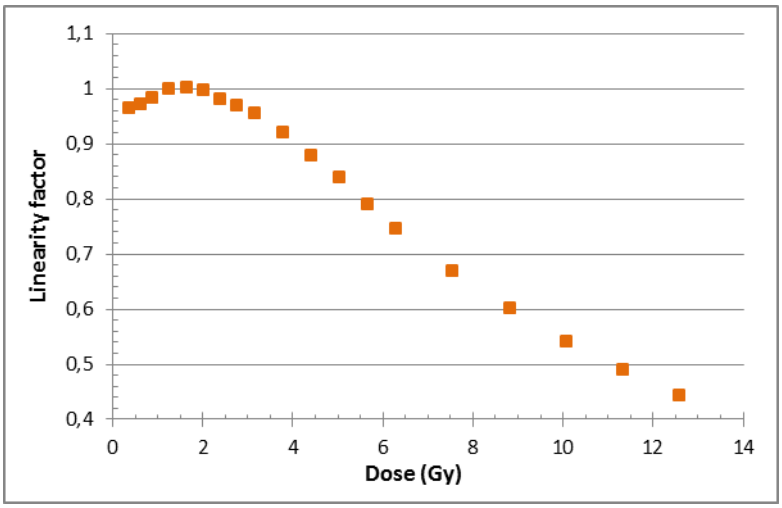

Figure 5.24. Linearity factor (f(D)) for the data points of the linearity test of the single crystal shown in Figure 5.23.. Estimations were done using as a reference the dose response obtained at 1,26 Gy.

Figure 5.24 shows that the OSL response in Figure 5.23. is linear up to about 3 Gy considering a variation of 5% of the linearity factor. Beyond 3 Gy the OSL response starts a sublinear regimen indeed. An explanation of the early decrease of the OSL response of the single crystal may be again related to the weak range of beta particles when interacting with the thick detector material.

The energy of the beta particles emitted by the $^{90}Sr/^{90}Y$ source are not energetic enough to penetrate the whole volume of the detector and, instead of this, they rapidly lose their energy and are stopped near the surface of the crystal (the single macro crystal). As the beta particles only penetrate the surface, only the crystal defects in the vicinity of the surface of the detector are excited by the radiation. Then, after a certain dose, these defects start becoming full and then there are no more empty traps to hold the excited charges. This causes the saturation of the OSL signal because the charge carriers excited by the beta particles will not be trapped and will not be able to emit the luminescence when a stimulated with light. This saturation is thus associated to the complete filling of defects near the surface.

Besides this, when shorter integration times were used to estimate the initial OSL intensity, a strong supralinear behaviour was observed almost all over the tested dose range. In fact, the supralinearity of the single crystal was much more prominent than the observed in general for micro crystals at short integration times. This is because changes in the OSL decay curves are more accentuated for the single crystal than for Luxel and powder detectors (see Figure 5.25). Then, using this type of detector with short stimulation times with beta and other low penetrating source is less advantageous than using thinner detectors like Luxel and powder detectors.

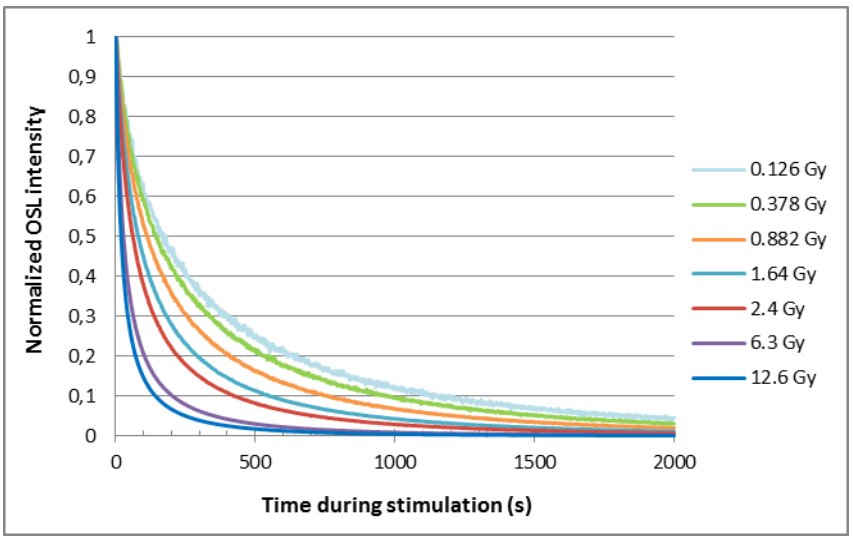

Figure 5.25. Changes in the shape of the OSL curve depending on the delivered dose to the single crystal. The OSL was stimulated with blue light at 3% of the maximum power (~ 1.5 mW.cm^{-2}). OSL curves correspond to normalized values.

5.4 Comparison of detectors

Finally, a comparison of the dosimetric properties of the three forms of Al_2O_3:C detectors summarizes some important results presented in the last sections.

In terms of the OSL response to beta radiation, both Luxel detectors and powder samples presented a linear behaviour from 126 mGy to up to about 10 Gy with linearity factors varying less than 5% in the same range. This behaviour is achieved if the optimal integration time was used to estimate the integrated OSL intensity. For the experimental conditions used here, the optimal integration time for Luxel detectors was around 700s (11-12 min) while for powder detectors it was of 10s. When shorter times were used in the calculations, in both cases the dose response rapidly became supralinear and the dose range with linear response was more limited. Then, in the practice a powder detector similar to those used here would present the advantage of a fast readout time without sacrificing the linearity of the OSL response. Besides it, shorter periods of exposure to blue light are needed to completely bleach the prepared powder detectors. Both points of powder detectors would be interesting for a real time in-vivo dosimetric system where fast OSL measurements are desired.

Respect to the single crystal, its OSL response to beta particles was linear only until 3 Gy of beta particles. In addition, it presents more pronounced changes in the shape of the OSL curve depending on the absorbed dose, which means that a stronger supralinearity in the dose response is observed if shorter stimulation times are used to estimate the integrated OSL intensity. Then, this detector is more appropriate for applications using longer stimulation times and more limited for fast measurements.

Regarding the dose response to gamma rays, powder detectors showed a linear response over a wider dose range than Luxel detectors. For the first ones a linear response was seen from 100 mGy up to 10 Gy, while for the second ones it was seen until about 7,5 Gy. However, since linearity tests using gamma photons presented higher dispersions in the results, it would be reasonable to corroborate these dose ranges by evaluating more absorbed doses while performing the test.

Besides this, gamma showed to be more efficient to excite powder detectors than beta particles, causing the emission of higher OSL intensities for a given delivered dose. However, the effect of increasing the concentration of powder per sample on the difference of the dose response between beta and gamma irradiated samples would be an interesting test to perform in the future, having in

mind that at higher concentrations of powder there are more probabilities that a higher number of electrons reachs the micro crystals before being stopped by the polymer (which is one of the causes of the difference between these OSL responses).

Respect to the spatial resolution achievable with each of the detectors used here, powder detectors are undoubtedly the ones that allow reducing the most the size of the detector. The single crystal is small enough (transversal area of 1 mm^2) to be coupled to an optical fiber but it is 2 millimetres long. Luxel detectors can be cut in different sizes from the Luxel tape but cannot be attached to an optical probe whether necessary. Besides this, powder samples can be made such as small as desired once it has been identified the appropriate procedure to measure the intended volume of powder-polymer compound.

In addition, in the case of powder samples, the shape and the amount of powder of the detector are parameters that can be chosen by the researcher/user according to his needs. For example, as occurred with the Apollo system, if the detection unit of a reader system is being saturated by the OSL signal of the detector and the stimulating light cannot be lowered to avoid this effect, detectors with an appropriate concentration of powder can be prepared to control the emitted luminescence. The preparation of detectors following the basic protocol used here does not imply the use of expensive materials and equipment. Once having the powder and polymer and the instruments to prepare the drops of compound, a strong UV source is the only equipment necessary to complete the task.

Other dosimetric aspects tested in this work were the changes in the OSL sensitivity with the accumulated dose of the detectors and the fading of the OSL signal within the time elapsed between irradiation and readout.

Respect to variations in the OSL sensitivity, Luxel detectors presented sensitization of 10% to 50% for an accumulated beta dose of 22 Gy depending on the integration time used for the estimations, while prepared detectors showed a desensitization of about 40% to 50% for the same accumulated dose and a notable increase in sensitivity for accumulated doses between ~ 200 and 400 Gy. An accumulated dose of at least 190 Gy showed to improve the linearity of the dose response of powder detectors. The behaviour of Luxel detectors at accumulated doses higher than 28 Gy of beta was not inspected. This effect of sensitization and/or desensitization of detectors seemed to affect several of the tests performed during this project. Then, in a future work it is of prime importance to investigate the behaviour of the OSL sensitivity at higher doses for both types of detectors to see whether there is an accumulated dose above which the sensitivity of the detectors stabilizes.

Finally, regarding fading effects, preliminary results from the performed tests did not allow a definitive conclusion on the stability of the OSL signal after irradiation. Results obtained from fading tests carried out inside the Risø reader showed an abnormal behaviour in which the OSL signal of both Luxel and powder detectors increases with the time elapsed between irradiation and readout. On the other hand, measurements taking the detectors out of the Risø during the time between irradiation and readout yielded dispersed results without any preferential behaviour of the OSL signal.

6 CONCLUSION

This work presented some dosimetric aspects of the OSL response of Al_2O_3:C powder detectors for beta and gamma radiation, demonstrating the possibilities of use of such an OSLD in the field of medical dosimetry.

Al_2O_3:C powder OSLDs were prepared in the form of flattened drops of 2-3 mm in diameter by mixing the material with a photo-curable polymer that hardens when illuminated with strong UV light. The polymer showed to be appropriate to be used as a matrix for the powder since no OSL sensitivity was detected when it was irradiated with different beta doses.

A first test using powder samples with the same volume of compound but different concentrations of powder showed that the OSL response of samples increases with the amount of powder used per detector indeed. From this test, the minimum amount of powder necessary to perform a dosimetric measurement with the Risø reader was estimated. It was found that 1 µg of Al_2O_3:C powder per detector is needed if doses equal or above 1,26 Gy of beta are supposed to be measured with the detector. To measure doses equal or higher than 100 mGy of beta, 10 µg of powder should be used in each detector. These minimum amounts of powder are not limited by the powder itself, but by the sensitivity of the PMT in the Risø reader. Despite of that, the small amounts of powder that were found to be necessary to perform a dosimetric measurement reveal the valuable high sensitivity of the Al_2O_3:C powder to ionizing radiation.

On the other hand, several dosimetric properties of powder samples were assessed and were compared with those obtained for Luxel detectors and a single crystal. This preliminary study showed that in terms of linearity, powder detectors have an OSL dose response for $^{90}Sr/^{90}Y$ beta radiation comparable to that of Luxel detectors. Powder samples exhibit a linear behaviour from 126 mGy to about 10 Gy, while Luxel detectors do it until about 9 Gy. With respect to the single crystal, powder detectors presented an extended dose range with linear OSL response, since the first one started exhibiting a strong sublinearity from about 3 Gy probably due to the charged nature of beta radiation. Regarding the OSL response to ^{60}Co gamma rays, the dose range with linear behaviour was wider for powder samples (~ 0,1 - 10 Gy) than for Luxel detectors (~ 0,1 - 7,5 Gy), but further tests have to be done to corroborate the dose ranges. These results show that the dose range of powder detectors with linear OSL response to beta and gamma radiation is wide enough to account for the doses commonly measured in personal and medical dosimetry.

Apropos of linearity, during this work it was highlighted the importance of using the linearity factor if a precise assessment of the degree of linearity of the dose response is required. Sometimes this factor evidenced the presence of a nonlinear behaviour at doses where the OSL response seemed to be linear. Also, the choice of an appropriate integration time to estimate the integrated OSL intensity was shown to be determinant in the behaviour of the dose response curve. When using short times the OSL response usually presents a strong supralinearity, while when using long integration times the OSL response tends to exhibit an early sublinear behaviour. Then, the optimal integration time for each detector and experimental readout conditions should be sought so that the widest dose range with linear OSL response is achieved. Due to their lower concentration of defects, optimal integration times and bleaching times of powder detectors were always shorter than those of Luxel detectors and single crystal. This aspect represents an advantage of powder detectors respect to the others when used in real time in-vivo dosimetric systems where fast OSL measurements are desired.

Comparing beta and gamma irradiations, the OSL response of powder samples irradiated with ^{60}Co gamma rays was higher than that one of samples irradiated with $^{90}Sr/^{90}Y$ beta rays. Similarly as occurred with the single crystal, part of this effect may be due to the charged nature of beta radiation. Further measurements using X-rays and gamma photons of different energies should be performed to know how energy dependent are the prepared detectors.

About changes in the OSL sensitivity with the accumulated dose, powder and Luxel detectors showed opposite effects. For accumulated doses below 30 Gy of beta powder samples exhibited a decrease in their sensitivity while Luxel detectors were sensitized. Then, at higher doses powder samples showed sensitization too. Nevertheless, any of these effects are desired in an OSL dosimetric detector since it means that a calibration curve has to be done each time that the detector is used. In this study this adverse effect seemed to affect several of the results of the performed tests. From now on it has to be investigated whether the sensitivity can be stabilized by giving the detectors a higher accumulated dose before their use.

Respect to fading effects, preliminary results from the performed tests did not yield a definitive conclusion on the stability of the OSL signal after irradiation. This test has to be performed again after having solved the inconveniences of changes of OSL sensitivity with accumulated dose and checked the repeatability of the OSL measurements using the Risø reader.

Finally, powder detectors possess two important advantages over the other two types of Al_2O_3:C detectors. First one is that powder detectors can attain higher spatial resolution than Luxel and single crystal detectors since the drops of compound powder+polymer can be made such as small as desired once it has been identified the appropriate procedure to measure the small volumes. The other one is related to the flexibility to prepare your own detectors using your own protocol. As mentioned before, when preparing the powder samples, the amount of powder used in the detector and its shape are parameters that can be chosen by the researcher according to his needs.

From now on, future work should focus on carrying out some other tests to refine the results obtained during this work and to go farther in the study of the dosimetric properties of the Al_2O_3:C powder detectors. The following measurements are proposed for this purpose:

- Test of changes in OSL sensitivity for a wider accumulated dose range of beta to determine whether there is an accumulated dose above which the sensitivity stabilizes. Then, the same test using X-rays or gamma photons should be performed.
- Assessment of the repeatability of the OSL measurements with the Risø reader using different experimental conditions to account for the precision of the measurements.
- Energy dependence tests using X-rays and gamma photons of different energies.
- Evaluation of the OSL response to beta rays of detectors with higher concentrations of powder.
- Repetition of the fading tests using samples with stabilized OSL sensitivity.
- Test of the influence of other types of bleaching procedures in the OSL response of Luxel and powder samples.
- Influence of environmental conditions like temperature and humidity.

Going farther, additional work should be spent in improving the protocol to prepare the samples and in determining the real amount of powder within the detectors.

The proposed future tests will be performed later since a work contract at SCK•CEN for one year was obtained at the end of the internship. Finally, from the results presented in this report, an article will be written and this one will be submitted to a peer-reviewed international scientific journal.

Acknowledgement

I would like to specially thank my external supervisor Luana de Freitas Nascimento, because of her great patient, her friendliness and her valuable dedication to help me and guide me during all my internship experience.

I would also like to thank SCK•CEN for providing me the opportunity to undertake this Master internship project in its facilities in Mol, and more specifically to the Radiation protection, Dosimetry and Calibration expert group for its warm and considerate welcome.

I am grateful with Dr. Mark Akselrod (Landauer Crystal growth division, Stillwater) for providing the Al_2O_3:C powder and single crystal and with the European Commission for providing part of the funding to cover my living expenses during these six months.

References

Agersnap-Larsen N. Dosimetry based on Thermally and Optically Stimulated Luminescence [Report] / Riso National Laboratory. - Denmark : Riso National Laboratory, 1997. - pp. 79-81.

Akselrod M.S. [et al.] Highly sensitive thermoluminescent anion-defect α-Al2O3:C single crystals detectors [Journal] // Radiation Protection Dosimetry. - 1990. - Vol. 33. - pp. 119-122.

Akselrod M.S. and McKeever S.W.S. A radiation dosimetry method using pulsed optically stimulated luminescence [Journal] // Radiation Protection Dosimetry. - 1999. - 3 : Vol. 81. - pp. 167-176.

Akselrod M.S., Bøtter-Jensen L. and McKeever S.W.S. Optically stimulated luminescence and its use in medical dosimetry [Journal] // Radiation Measurements. - 2007. - Vol. 41. - pp. S78-S99.

Akselrod M.S., V.S. Kortov and Gorelova E.A. Preparation and properties of a-Al2O3:C [Journal] // Radiation Protection Dosimetry. - 1993. - Vol. 47. - pp. 159-164.

Andersen C. E. [et al.] Temperature coefficients for in vivo RL and OSL dosimetry using Al2O3:C [Journal] // Radiation Measurements. - 2008. - 2-6 : Vol. 43. - pp. 948-953.

Attix F. H. Introduction to Radiological Physics and Radiation Dosimetry [Book]. - New York : Wiley, 1986. - p. 279.

Aznar M.C. [et al.] Real-time optical-fibre luminescence dosimetry for radiotherapy: physical characteristics and applications in photon beams [Journal] // Physics in Medicine and Biology. - 2004. - Vol. 49.

Bøtter-Jensen L. [et al.] Al2O3:C as a sensitive OSL dosemeter for rapid assessment of environmental photon dose rates [Journal] // Radiation Measurements. - 1997. - 2 : Vol. 27. - pp. 295-298.

Bøtter-Jensen L. and McKeever S. W. S. Optically stimulated luminescence dosimetry using natural and synthetic materials [Journal] // Radiation Protection Dosimetry. - 1996. - Vol. 65. - pp. 273-280.

Bøtter-Jensen L., McKeever S. W. S. and Wintle A. G. Optically Stimulated Luminescence Dosimetry [Book]. - Amsterdam : Elsevier B.V., 2003. - pp. 6, 75.

Cygler J.E. and Yukihara E.G. Optically stimulated luminescence (OSL) dosimetry in radiotherapy [Conference] // Clinical Dosimetry Measurements in Radiotherapy (AAPM 2009 Summer School) / ed. Rogers D.W.O. and Cygler J.E.. - [s.l.] : Medical Physics Publishing , 2009.

de Freitas Nascimento L. Dosimetria usando Luminescência Opticamente Estimulada: aplicações, propiedades físicas e caracterização de materiais dosimétricos [Report] / Universidade de São Paulo. - São Paulo : Universidade de São Paulo, 2007. - p. 21.

Evans B.D. A review of the optical properties of anion lattice vacancies, and electrical conduction in α-Al2O3: their relation to radiation-induced electrical degradation [Journal] // Journal of Nuclear Materials. - 1995. - Vol. 219. - pp. 202–223.

Gaza R. [et al.] A fiber-dosimetry method based on OSL from Al2O3:C for radiotherapy applications [Journal] // Radiation Measurements. - 2004. - Vol. 38. - pp. 809 –812.

Gore E. M. [et al.] Pulmonary function changes in long-term survivors of bone marrow transplantation [Journal] // International Journal of Radiation Oncology*Biology*Physics. - 1996. - 1 : Vol. 36. - pp. 67-75.

Huston A. L. [et al.] Remote optical fiber dosimetry [Journal] // Nuclear Instruments and Methods in Physics Research Section B. - 2001. - 1-2 : Vol. 184. - pp. 55-67.

Jursinic P. A. Changes in optically stimulated luminescent dosimeter (OSLD) dosimetric characteristics with accumulated dose [Journal] // Medical Physics. - 2010. - 1 : Vol. 37.

Jursinic P. A. Characterization of optically stimulated luminescent dosimeters, OSLDs, for clinical dosimetric measurements [Journal] // Medical Physics. - 2007. - 12 : Vol. 34.

M. S. Akselrod V. S. Kortov, D. J. Kravetsky and V. I. Gotlib Highly sensitive thermoluminescent anion-defect a-Al2O3:C single crystal detectors [Journal] // Radiation Protection Dosimetry. - 1990. - Vol. 33. - pp. 119-122.

Mangili P. [et al.] In-vivo dosimetry by diode semiconductors in combination with portal films during TBI: reporting a 5-year clinical experience [Journal] // Radiotherapy and Oncology. - 1999. - 3 : Vol. 52. - pp. 269-276.

Marckmann C. J. [et al.] Optical fibre dosemeter systems for clinical applications based on radioluminescence and optically stimulated luminescence from Al2O3:C [Journal] // Radiation Protection Dosimetry. - 2006. - 1-4 : Vol. 120. - pp. 28-32.

Markey B. G. [et al.] The temperature dependence of optically stimulated luminescence from Al2O3 :C [Journal] // Radiation Protection Dosimetry. - 1996. - Vol. 65. - pp. 185–189.

Markey B. G., Colyott L. E. and McKeever S. W. S. Time-resolved optically stimulated luminescence from α-Al2O3:C [Journal] // Radiation Measurements. - 1995. - Vol. 24. - pp. 457–463.

McKeever S. W. S. Optically stimulated luminescence dosimetry [Journal] // Nuclear Instruments and Methods in Physics Research Section B. - 2001. - 1-2 : Vol. 184. - pp. 29-54.

McKeever S. W. S., Moscovitch M. and Townsend P. D. Thermoluminescence Dosimetry Materials: Properties and Uses. - Ashford : Nuclear Technology Publishing, 1995.

Miller S. D. [et al.] A high-precision, tissue-equivalent dosimeter for nuclear accident and radiation oncology applications based on optically stimulated luminescence (OSL) in Al2O3:C [Journal] // Radiation Measurements. - 2008. - 2-6 : Vol. 43. - pp. 875-878.

N. Agersnap-Larsen Dosimetry based on Thermally and Optically Stimulated Luminescence [Report] / Riso National Laboratory. - Denmark : [s.n.], 1997. - pp. 79-81.

Polf J.C. [et al.] Real-time luminescence from Al2O3 fiber dosimeters [Journal] // Radiation Measurements. - 2004. - Vol. 38. - pp. 227–240.

Pradhan A.S., Lee J.I. and Kim J.L. Recent developments of optically stimulated luminescence materials and techniques for radiation dosimetry and clinical applications [Journal] // Journal of Medical Physics. - 2008. - 3 : Vol. 33. - pp. 85–99.

Reft C. S. The energy dependence and dose response of a commercial optically stimulated luminescence detector for kilovoltage photon, megavoltage photon, and electron, proton, and carbon beams [Journal] // Medical Physics. - 2009. - 5 : Vol. 36.

Schembri V. and Heijmen B. J. M. Optically stimulated luminescence (OSL) of carbon-doped aluminum oxide (Al2O3:C) for film dosimetry in radiotherapy [Journal] // Medical Physics. - 2007. - 6 : Vol. 34.

Summers G. P. Thermoluminescence in single crystal α-Al2O3 [Journal] // Radiation Protection Dosimetry. - 1984. - Vol. 8. - pp. 69-80.

Summers G. P. Thermoluminescence in single crystal α-Al2O3 [Journal] // adiation Protection Dosimetry. - 1984. - Vol. 8. - pp. 69-80.

Summers G. P. Thermoluminescence in single crystal α-Al2O3 [Journal] // Radiation Protection Dosimetry. - 1984. - Vol. 8. - pp. 69-80.

Umisedo N. K. [et al.] Comparison between blue and green stimulated luminescence of Al2O3:C [Journal] // Radiation Measurements. - 2010. - Vol. 45. - pp. 151–156.

Yukihara E. G. [et al.] Effect of high-dose irradiation on the optically stimulated luminescence of Al2O3:C [Journal] // Radiation Measurements. - 2004. - 3 : Vol. 38. - pp. 317-330.

Yukihara E. G. [et al.] Medical applications of optically stimulated luminescence dosimeters (OSLDs)", Radiation Measurements [Journal]. - 2010. - Vol. 45. - pp. 658–662.

Yukihara E. G. and McKeever S. W. S. Ionisation density dependence of the optically and thermally stimulated luminescence from Al2O3:C [Journal] // Radiation Protection Dosimetry. - 2006b. - 1-4 : Vol. 119. - pp. 206-217.

Yukihara E. G. and McKeever S. W. S. Optically Stimulated Luminescence: Fundamentals and Applications [Book]. - [s.l.] : Wiley, 2011. - pp. 78, 83-88, 123-126, 222-224.

Yukihara E.G. [et al.] Application of the optically stimulated luminescence (OSL) technique in space dosimetry [Journal] // Radiation Measurements. - 2006a. - 9-10 : Vol. 41. - pp. 1126-1135.

Yukihara E.G. and McKeever S. W. S. Spectroscopy and optically stimulated luminescence of Al2O3:C using time-resolved measurements [Journal] // Journal of Applied Physics. - 2006c. - 8 : Vol. 100.